

Few-body insights into the Quantum Hall problem

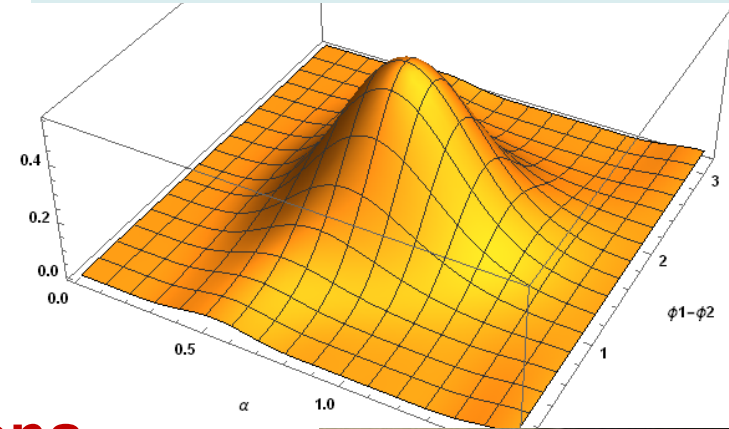
Chris Greene, Kevin Daily, Bin Yan, and Rachel Wooten, Purdue

In this talk:

- Formulate the 2D system of electrons on the plane in a B-field using collective hyperspherical coordinates
- Show a correlation between
- fractional quantum Hall states and
- states of exceptional degeneracy
- *Wild, unrestrained speculations on future directions for this line of research will be offered...*

→ Phys. Rev. B **92**, 125427 (2015)

3 particle Laughlin $1/3$ state plotted versus 2 hyperangles



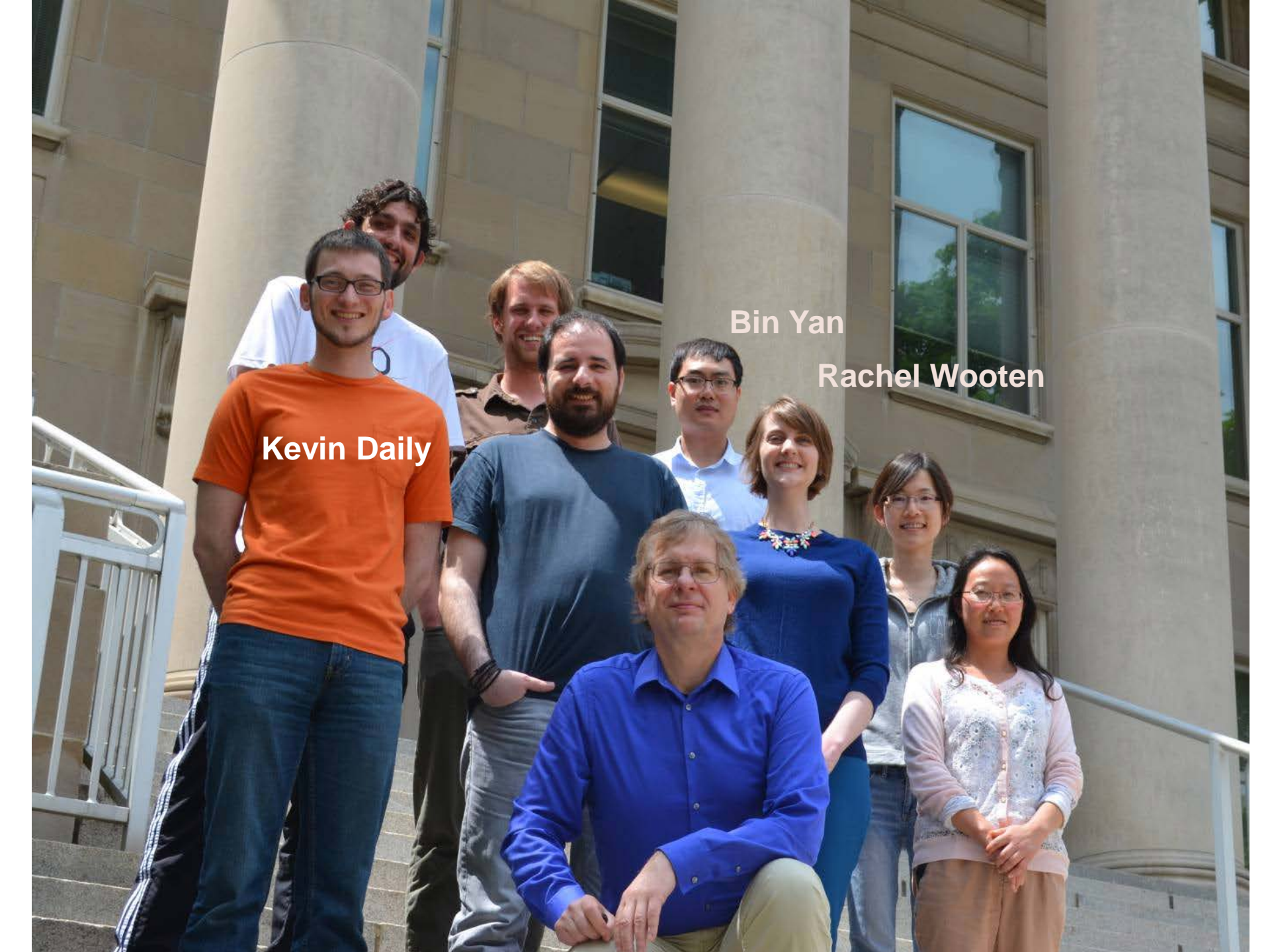
Bin Yan



Kevin Daily



Rachel Wooten



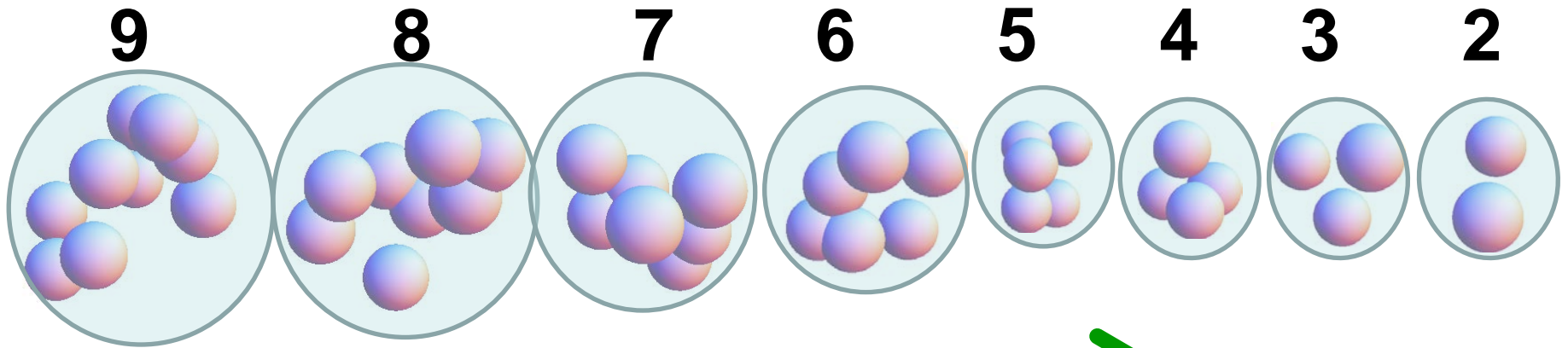
Kevin Daily

Bin Yan

Rachel Wooten

From few to many – How can we understand the universality?

$$H = \underbrace{\sum_{i=1}^N \frac{p_i^2}{2m_i}}_{N \text{ repulsive terms } > 0} + \underbrace{\sum_{i < j} V(r_{ij})}_{\substack{\uparrow \frac{N(N-1)}{2} \\ \text{attractive terms } < 0}}$$



INCREASING ATTRACTION (a gets more negative) →

**Extensions of Universal Efimov Physics
to $N > 3$ Bosons in 3D**

Fermi Systems in Nature

- Condensed matter physics:
 - Electrons in a crystal.
 - Fractional quantum Hall effect
 - Cooper pairs.
 - High T_c superconductivity.
- Nuclear physics/astrophysics:
 - Low density neutron matter (inner crust of neutron stars).
- Atomic physics:
 - Composite fermions (atomic gas).
 - Essentially no impurities.
 - Control of interaction strength and confinement.
 - Opportunity to study few-body and many-body physics.

The Fractional Quantum Hall Effect

J. P. EISENSTEIN AND H. L. STORMER

SCIENCE, VOL. 248 1990

1510

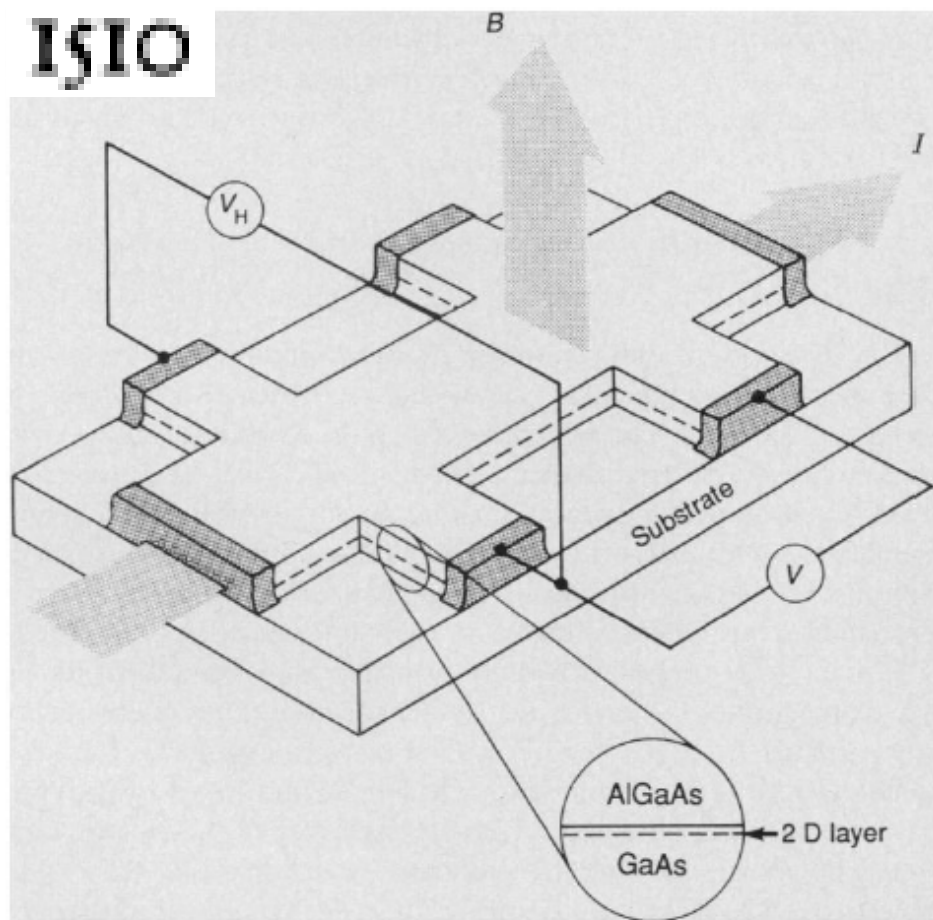


Fig. 1. A typical Hall bar sample. The structure is formed by chemically etching away unwanted material. The dotted line indicates the 2-D electron gas at the interface between gallium arsenide (GaAs) and aluminum gallium arsenide (AlGaAs). The magnetic field B and electrical current I are shown,

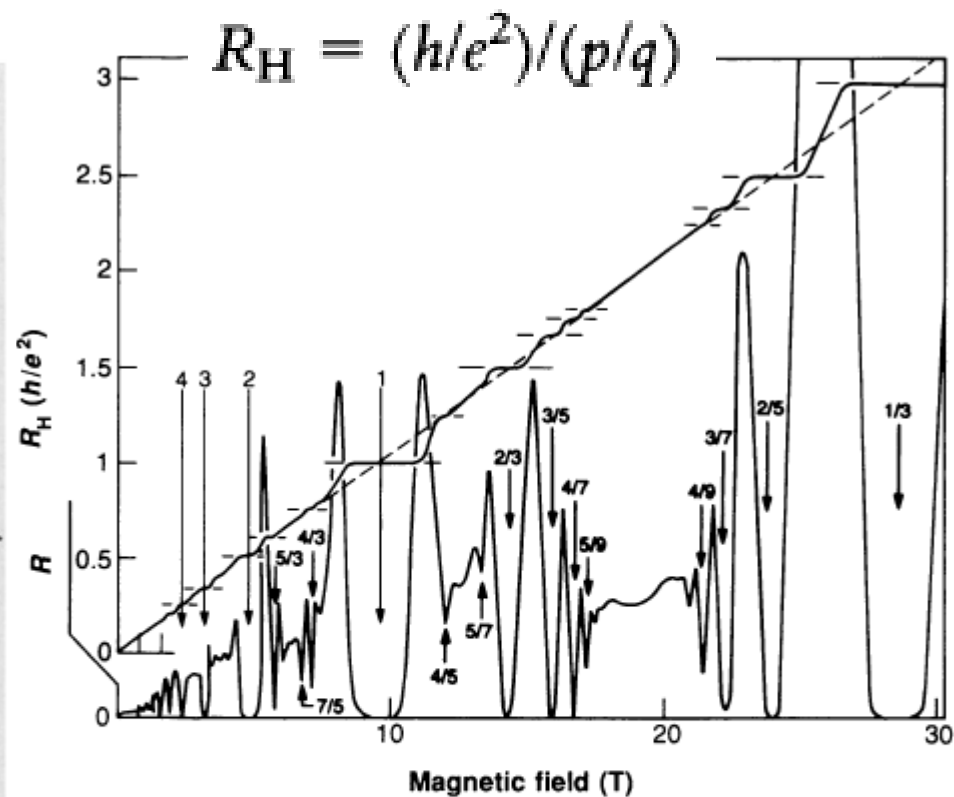


Fig. 2. Composite view showing the Hall resistance R_H and longitudinal resistance R of a 2-D electron gas versus magnetic field. The diagonal dashed line passing through the R_H trace represents the classically expected Hall resistance for this sample. For each of the plateaus in R_H there is an associated minimum in R . The numbers give the value of p/q determined from the value of R_H on the plateaus. While some of the p/q values are integers, the great majority are fractions. Note in particular the “1/3 state” at the far right. This most prominent example of the fractional quantum Hall effect exhibits a Hall plateau at $R_H = (h/e^2)/(1/3) = 3h/e^2$.

1983 Laughlin PRL:
3050 citations as of
today

Motivations

arXiv:1504.07884
Phys. Rev. B **92**, 125427 (2015)

Microscopic origin of the fractional QHE states

Can they emerge systematically without guessing wavefunctions?

What are quasi-particles?

How many electrons make up a quasi-particle, and how do their fractional charge and unusual statistics emerge?

Do properties of the non-interacting 2D free electron gas with no interactions determine whether a given filling factor yields a measurable FQHE state?

Whereas the full many-body Schroedinger equation is a linear PDE, many-body treatments such as mean-field theory are nonlinear. How can this linear \leftrightarrow nonlinear relationship be understood more deeply?

Since the FQHE is heralded as the prototype STRONGLY CORRELATED SYSTEM, can insights emerge from describing the system in COLLECTIVE COORDINATES rather than as independent electrons?

Physics is often about exploring phenomena from different points of view, i.e. different TOOLKITS. One example is the *“few-body hyperspherical toolkit”*

First of all, note that there have been many notable successes of hyperspherical coordinate treatments by Macek, Fano, Lin, and others, especially in the Fano school:

Fano Group PhD theses using hyperspherical coordinates:

Ravi Rau, 1971

Chii-Dong Lin, 1974

C H Greene, 1980

Shinichi Watanabe, 1982

Michael Cavagnero, 1984

John Bohn, 1992

These followed and built to some extent on the formulation developed initially by Joe Macek, a project started when he was Fano's postdoc in the late 1960s.

Some recent successes also include the treatment of 3-body and 4-body recombination processes and Efimov physics (CHG, Physics Today 2010)

Some successes of the adiabatic hyperspherical representation:

1. Prediction that the Efimov effect should be observable using variable scattering lengths that can be controlled for ultracold atoms
2. Extensions of Efimov physics to describe universal states and recombination processes for 4 bosonic atoms
3. Treatment of the few-body systems that arise in the BCS-BEC crossover problem for a fermionic gas with two spin components (e.g. dimer-dimer and atom-dimer scattering properties)
4. Many-body applications to macroscopic numbers of bosons in a Bose-Einstein condensate, or fermions in a degenerate Fermi gas.

Many PhD students and postdocs have contributed to these developments: Hossein Sadeghpour, Brett Esry, Jim Burke, Jose D’Incao, Jia Wang, Doerte Blume, Seth Rittenhouse, Javier von Stecher, Viatcheslav Kokoouline, and at Purdue: Kevin Daily, Rachel Wooten, Bin Yan, Jesus Perez-Rios

Strategy of Macek's adiabatic hyperspherical representation: convert the partial differential Schroedinger equation into an infinite set of coupled ordinary differential equations:

To solve: \longrightarrow
$$\left[-\frac{1}{2\mu} \frac{\partial^2}{\partial R^2} + \frac{\Lambda^2}{2\mu R^2} + V(R, \theta, \varphi) \right] \psi_E = E \psi_E$$

First solve the fixed-R Schroedinger equation, for eigenvalues $U_n(R)$:

$$\left[\frac{\Lambda^2}{2\mu R^2} + \frac{15}{8\mu R^2} + V(R, \theta, \varphi) \right] \Phi_\nu(R; \Omega) = U_\nu(R) \Phi_\nu(R; \Omega)$$

Next expand the desired solution into the complete set of adiabatic eigenfunctions

\longrightarrow
$$\psi_E(R, \Omega) = \sum_\nu F_{\nu E}(R) \Phi_\nu(R; \Omega)$$

And the original T.I.S.Eqn. is transformed into the following set which can be truncated on physical grounds, with the eigenvalues interpretable as adiabatic potential curves, in the Born-Oppenheimer sense.

\swarrow

$$\left[-\frac{1}{2\mu} \frac{d^2}{dR^2} + U_\nu(R) \right] F_{\nu E}(R) - \frac{1}{2\mu} \sum_{\nu'} \left[2P_{\nu\nu'}(R) \frac{d}{dR} + Q_{\nu\nu'}(R) \right] F_{\nu' E}(R) = E F_{\nu E}(R)$$

Joe Macek's (1968 JPB) adiabatic hyperspherical picture gave insight into why only one series of autoionizing states is seen in He photoabsorption near the $n=2$ threshold, instead of three.

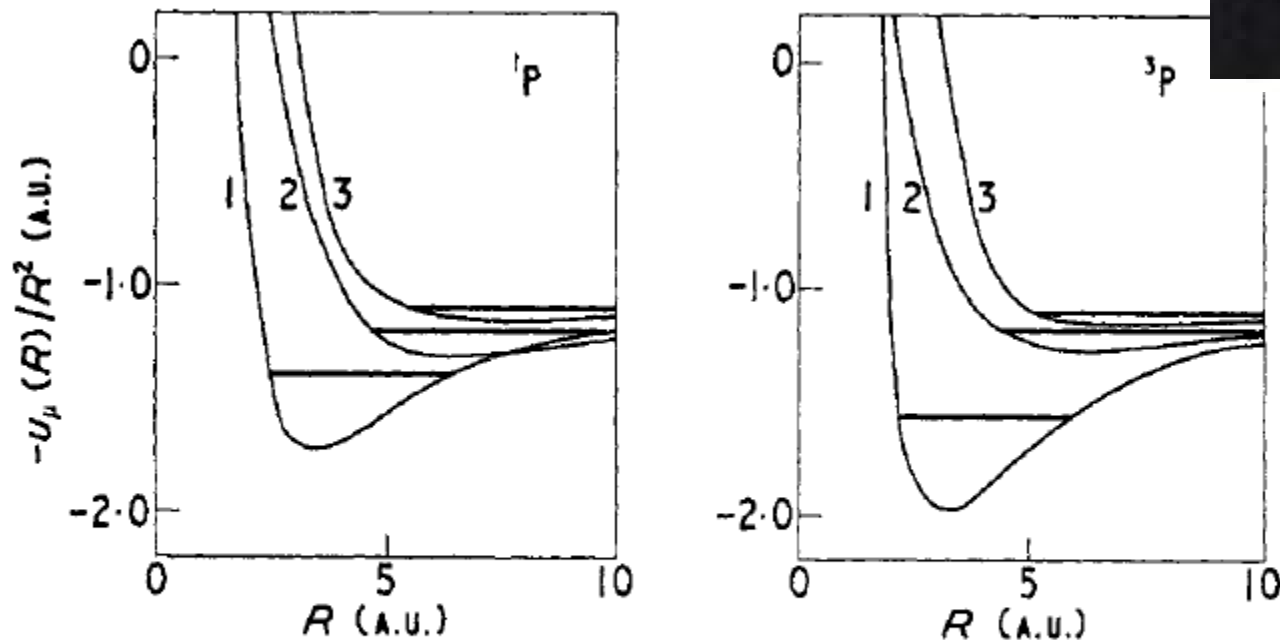


Figure 1. Graphs of $-U_\mu(R)/R^2$ against R for $^1S^e$, $^3S^e$, $^1P^o$ and $^3P^o$ cases. The 0th curve (ground state) is not shown. Positions of the lowest member of the Rydberg series of autoionizing states for each curve are marked by a horizontal line.

Table 6

Doubly excited states of He below the $N = 2$ hydrogenic threshold

	Complex rotation [72]		Feshbach projection [24]	
	$-E_r$ (Ry)	Γ (Ry)	$-E_r$ (Ry)	Γ (Ry)
$^1S^e(1)$	1.55574	0.00908	1.55607	0.00919
$^1S^e(2)$	1.243855	0.000432	1.24388	0.00049
$^1S^e(3)$	1.17985	0.0027	1.17984	0.00285
$^1S^e(4)$	1.09618	0.00009	1.09616	0.000177
$^1P^0(1)$	1.38627	0.00273	1.38632	0.002668
$^1P^0(2)$	1.194149		1.19414	8.56×10^{-6}
$^1P^0(3)$	1.1280	0.0006	1.12786	0.000735
$^1P^0(4)$	1.09385			
$^3P^0(1)$	1.520995	0.000594	1.52098	0.000654
$^3P^0(2)$	1.16930	0.00016	1.16925	0.0001919
$^3P^0(3)$	1.15806		1.15801	3.59×10^{-6}
$^3P^0(4)$	1.09768			

Table 9

Doubly excited resonances of He below the $N = 2$ He⁺ threshold

	Complex rotation ^a [71]	Experiments ^b	
		Hicks and Comer [140]	Gelebart et al. [141]
		E_r	
$^1S^e(1)$	57.848	57.82 ± 0.04	57.78 ± 0.03
$^3P^0(1)$	58.321	58.30 ± 0.03	58.29 ± 0.03
$^1P^0(1)$	60.154	60.13	60.13
$^1S^e(2)$	62.092	62.06 ± 0.03	62.10 ± 0.03
$^1S^e(3)$	62.962	62.94 ± 0.03	
$^3P^0(2)$	63.106	63.07 ± 0.03	63.06 ± 0.03
$^1P^0(3)$	63.668	63.65 ± 0.03	
		Γ	
$^1S^e(1)$	0.1235	0.138 ± 0.015	0.138 ± 0.015
$^3P^0(1)$	0.00808	<0.015	≈ 0.01
$^1P^0(1)$	0.03714	0.042 ± 0.018	0.041 ± 0.009
$^1S^e(3)$	0.0367	0.041 ± 0.010	

^a Resonances are measured from the ground state of helium atom ($E = -5.80744875$ Ry). The infinite rydberg (1 Ry = 13.605826 eV) was used for energy conversion.

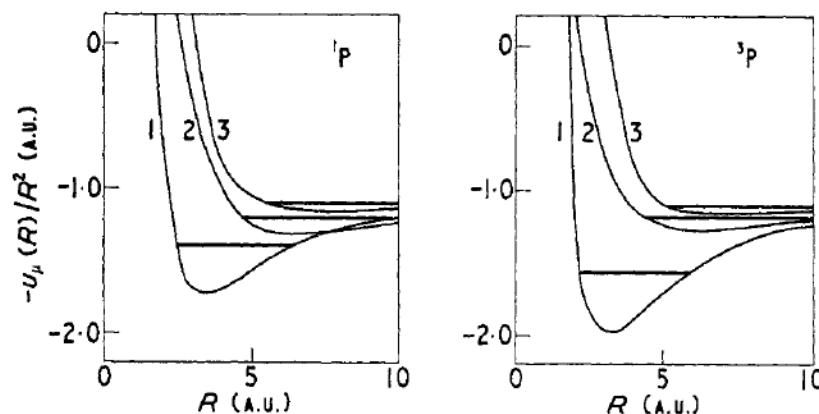


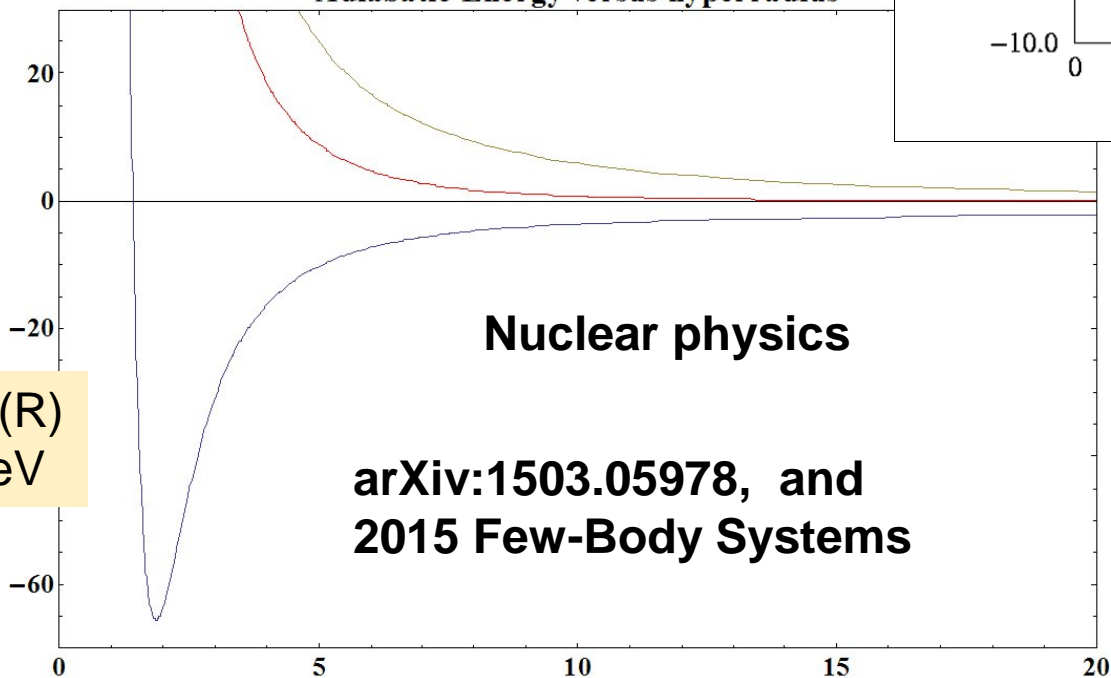
Figure 1. Graphs of $-U_\mu(R)/R^2$ against R for $^1S^e$, $^3S^e$, $^1P^0$ and $^3P^0$ cases. The 0th curve (ground state) is not shown. Positions of the lowest member of the Rydberg series of autoionizing states for each curve are marked by a horizontal line.

Universality, from nuclear scale energies to the chemical

Adiabatic potential curves for n+n+p, in collaboration with Alejandro Kievsky and Kevin Daily, nuclear physics on 10^6 eV scale (FBS 2015)

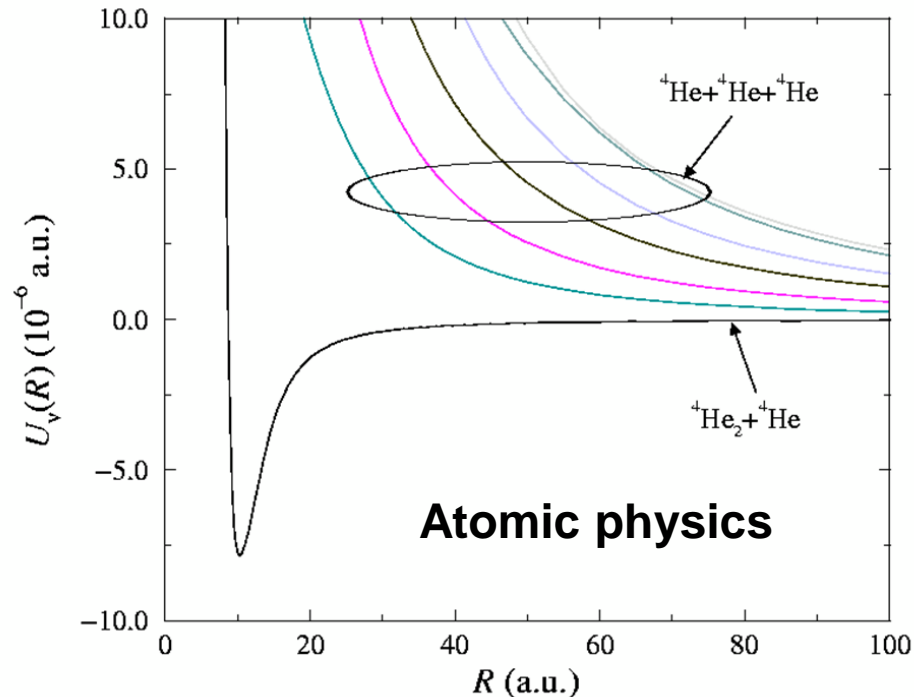


Adiabatic Energy versus hyperradius



arXiv:1503.05978, and 2015 Few-Body Systems

— hyperradius (fm)



3-atom hyperspherical potential curves for He+He+He on a 10^{-3} eV scale, looks very similar to the 3-nucleon potentials

Extensively used to understand universal Efimov physics

Here is our Hamiltonian, which we recast into hyperspherical coordinates in the usual way:

$$H = \sum_{i=1}^N \left(-\frac{\hbar^2}{2m} \nabla_i^2 + \frac{1}{2} m \omega^2 r_i^2 \right) + \sum_{i>j} U_{int}(\vec{r}_i - \vec{r}_j)$$

For a system of N atoms, with equal masses, one can define $M=Nm$ to be the total mass, and the kinetic energy operator then looks like:

$$\frac{-\hbar^2}{2M} \left(\frac{1}{R^{3N-1}} \frac{\partial}{\partial R} R^{3N-1} \frac{\partial}{\partial R} - \frac{\Lambda^2}{R^2} \right)$$

Here the hyperradius is defined as:

$$R = \left(\sum r_i^2 / N \right)^{1/2}$$

The adiabatic hyperspherical treatment treats the hyperradius R initially as an adiabatic coordinate like in Born-Oppenheimer theory, i.e. we diagonalize the H operator with R held fixed.

Some “prehistory” – hyperspherical BEC theory – many bosons

PHYSICAL REVIEW A

VOLUME 58, NUMBER 1

JULY 1998

Effective potentials for dilute Bose-Einstein condensates

John L. Bohn,* B. D. Esry,† and Chris H. Greene

Fermi's pseudopotential

$$\left\{ -\frac{\hbar^2}{2M} \left[\frac{\partial^2}{\partial R^2} - \frac{(3N-1)(3N-3)}{4R^2} - \frac{\Lambda^2}{R^2} \right] + \frac{1}{2} M \omega^2 R^2 + \sum_{i>j} \frac{4\pi\hbar^2 a}{m} \delta(\vec{r}_i - \vec{r}_j) - E \right\} R^{(3N-1)/2} \psi(R, \Omega) = 0.$$



Spherical trap approx.



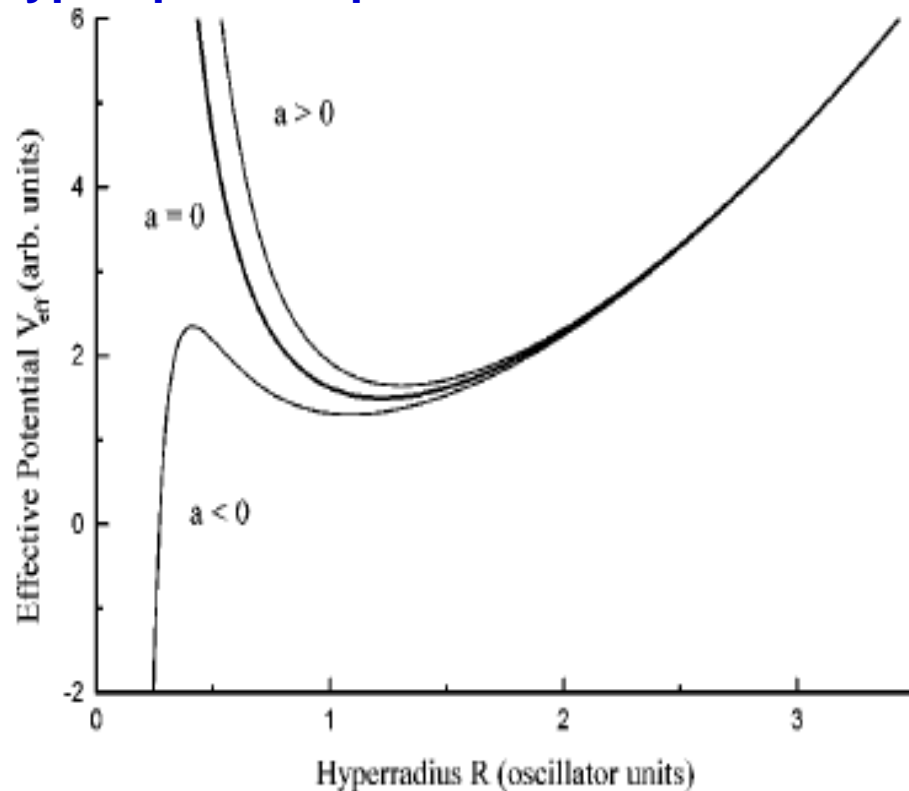
$$\left[-\frac{\hbar^2}{2M} \frac{d^2}{dR^2} + V_{\text{eff}}(R) \right] F(R) = E F(R),$$

described by the effective potential

$$V_{\text{eff}}(R) = \frac{\hbar^2}{2M} \frac{(3N-1)(3N-3)}{4R^2} + \frac{1}{2} M \omega^2 R^2 + \xi \sqrt{\frac{1}{2\pi} \frac{\hbar^2 a}{M} \frac{N^2(N-1)}{R^3}}.$$

$\xi \sim 1.837$

Hyperspherical potential curves for bosons



“Critical number for bosonic collapse”
is when:

$$\frac{Na_c}{L_{osc}} < -0.671$$

< -0.573 in HF/Gross-Pitaevskii theory

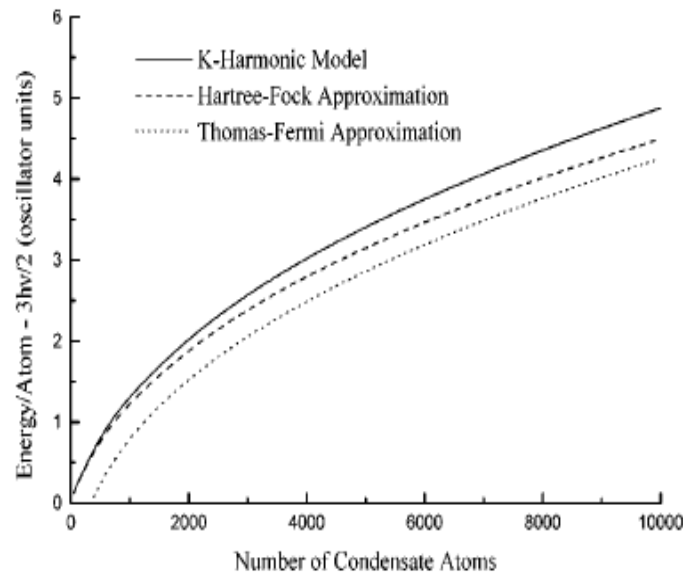
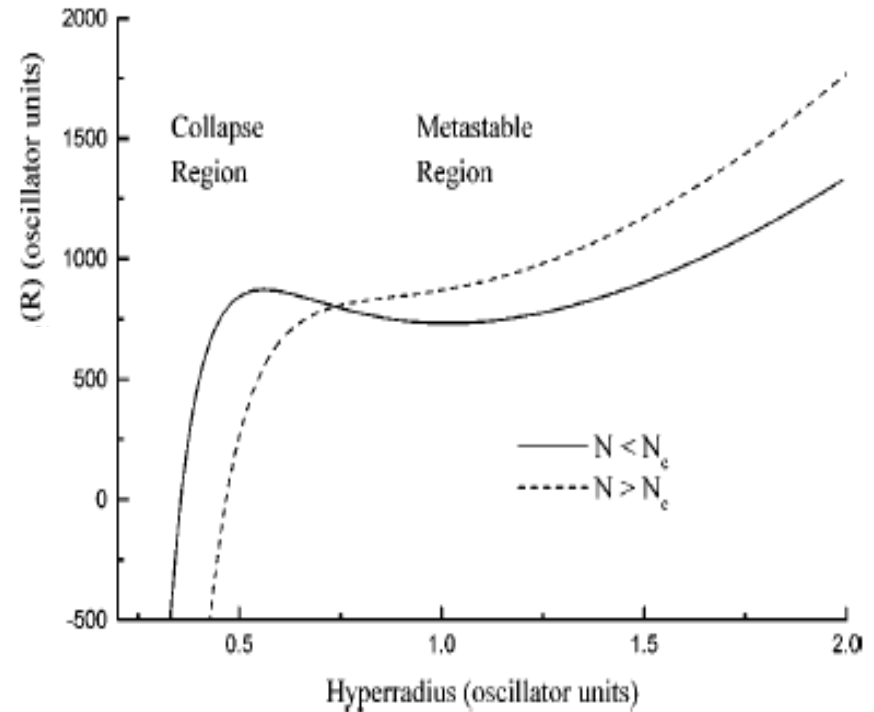
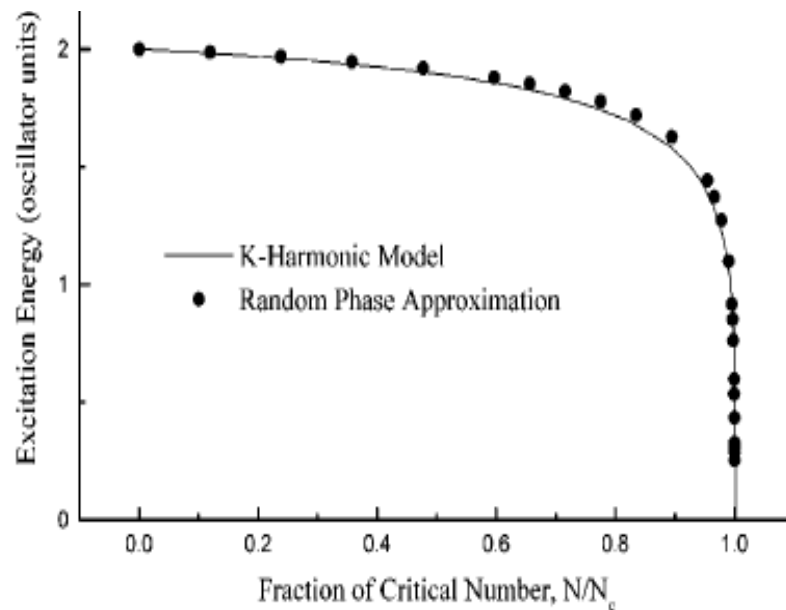
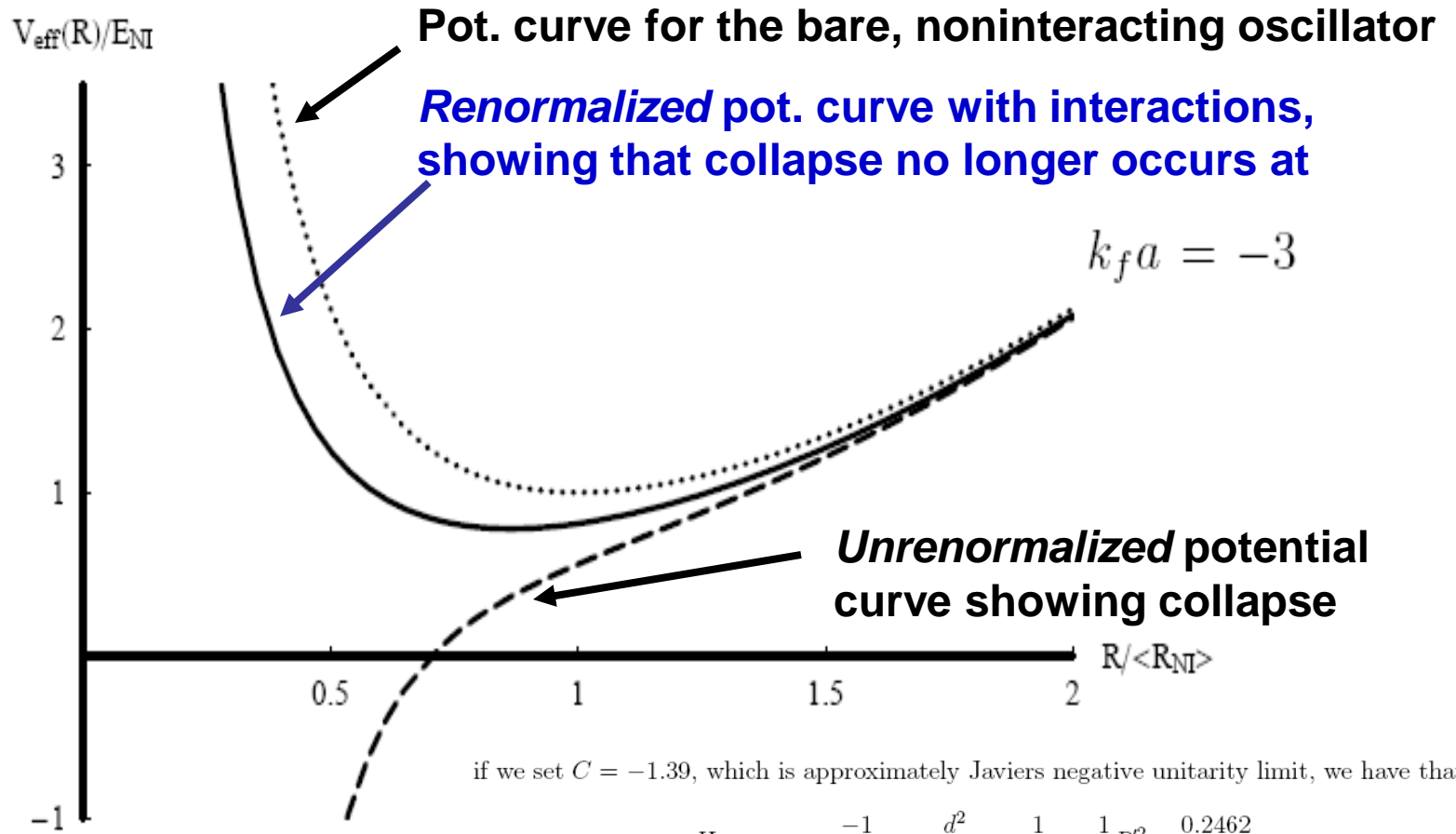


FIG. 2. Comparison of the K -harmonic, Hartree-Fock, and Thomas-Fermi estimates of the ground-state energy, for a condensate with $a=100$ bohr, and trap frequency $\nu=200$ Hz. The energy E_0 is plotted in the form $E_0/N - 3h\nu/2$, to emphasize the contribution of the energy beyond that in the noninteracting case.



Effect of renormalization on the adiabatic hyperspherical potential curve for a 2-component degenerate Fermi gas, in the large N limit:



$$\begin{aligned}
 H_{\text{eff}} &\rightarrow \frac{-1}{2E_{\text{NI}}\langle R^2 \rangle_{\text{NI}}} \frac{d^2}{dR^2} + \frac{1}{2R^2} + \frac{1}{2}R^2 - \frac{0.2462}{R^2} \\
 &= \frac{-1}{2E_{\text{NI}}\langle R^2 \rangle_{\text{NI}}} \frac{d^2}{dR^2} + \frac{0.254}{R^2} + \frac{1}{2}R^2
 \end{aligned}$$

FIG. 1: The non-interacting effective potential curve (dotted), and the effective potential curves for $k_f a = -3$ for the bare scattering length (dashed) and the renormalized effective scattering length (solid).

SINGLE PARTICLE HAMILTONIAN

Back to the quantum Hall problem:

→ Phys. Rev. B 92, 125427 (2015)

$$H = \frac{1}{2m_e} (-i\hbar\nabla + e\mathbf{A})^2 \quad \mathbf{A} = (B/2)(-y\hat{x} + x\hat{y})$$

$$H = -\frac{\hbar^2}{2m_e}\nabla^2 + \frac{e^2 B^2}{8m_e}(x^2 + y^2) + \frac{eB}{2m_e}L_z$$

$$E^{(1)} = \frac{1}{2}(2n + m + |m| + 1) \quad \leftarrow \text{Single particle energy levels}$$

Natural magnetic units
we use throughout:

Frequency:

$$\omega_c = eB/(m_e)$$

Energy: $\hbar\omega_c$

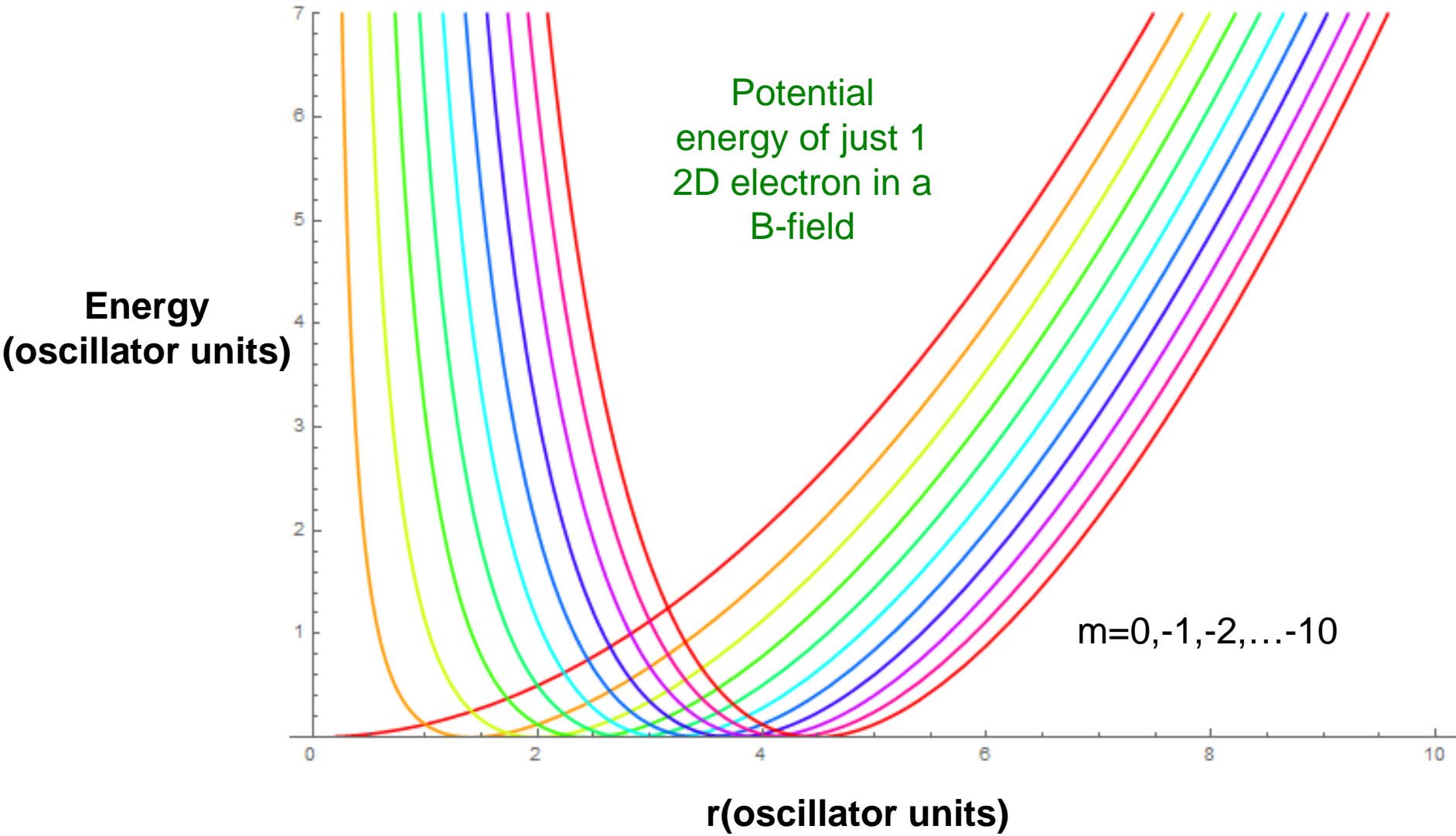
Length:

$$\lambda_0 = \sqrt{\frac{\hbar}{m_e\omega_c}}$$

$$H = -\frac{1}{2} \left\{ \frac{1}{r} \partial_r r \partial_r - \frac{L_z^2}{\hbar^2 r^2} \right\} + \frac{1}{8} r^2 + \frac{1}{2\hbar} L_z$$

Note: differs only by a
← constant from a
particle in a 2D trap
with B=0!

Single electron radial potential energy curves, $m=0, -1, \dots, -10$



Lowest 11 single-electron potential curves for an electron moving in two dimensions with a B-field transverse to the plane

N-BODY RELATIVE HAMILTONIAN

Now go to collective N-body coordinates

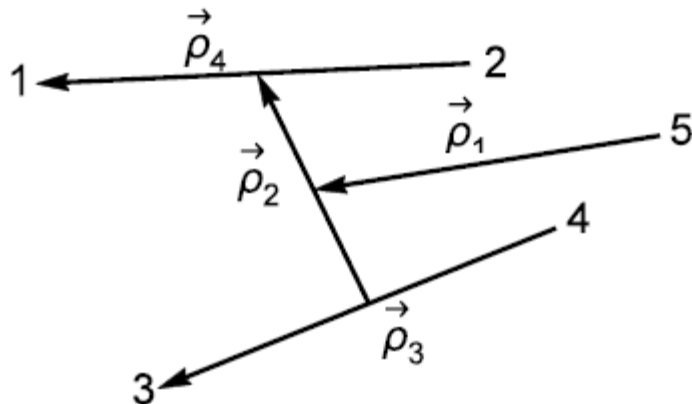
$$H_N = H_{CM} + H_{rel}$$

$$H_{rel} = -\frac{1}{2\mu} \sum_{j=1}^{N_{rel}} \nabla_j^2 + \frac{\mu}{8} \sum_{j=1}^{N_{rel}} (x_j^2 + y_j^2) + \frac{1}{2\hbar} \sum_{j=1}^{N_{rel}} L_{z_j}^{rel} \quad N_{rel} = N - 1$$

$$\mu = \left(\frac{1}{N}\right)^{1/N_{rel}} \quad \leftarrow \text{N-body reduced mass}$$

d=2N-2
dimensional
space, symmetry
group is O(2N-2)

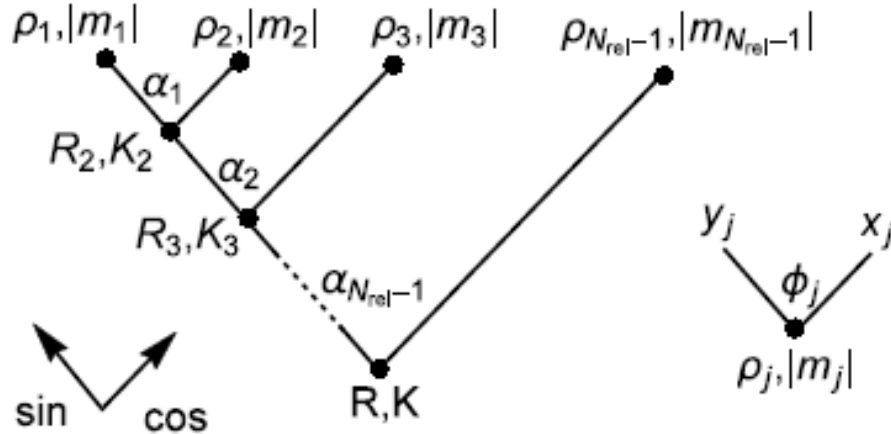
The 4 relative Jacobi vectors that characterize a 5-particle system in 2D:



Linear transformation matrix between the independent particle coordinates and the Jacobi relative+CM coordinates:

$$\begin{pmatrix} \rho_1 \\ \rho_2 \\ \rho_3 \\ \rho_4 \\ \rho_{CM} \end{pmatrix} = \begin{pmatrix} \sqrt{\frac{4/5}{\mu}} \times \{ \frac{1}{4} & \frac{1}{4} & \frac{1}{4} & \frac{1}{4} & -1 \} \\ \sqrt{\frac{1}{\mu}} \times \{ \frac{1}{2} & \frac{1}{2} & -\frac{1}{2} & -\frac{1}{2} & 0 \} \\ \sqrt{\frac{1/2}{\mu}} \times \{ 0 & 0 & 1 & -1 & 0 \} \\ \sqrt{\frac{1/2}{\mu}} \times \{ 1 & -1 & 0 & 0 & 0 \} \\ \frac{1}{5} \times \{ 1 & 1 & 1 & 1 & 1 \} \end{pmatrix} \begin{pmatrix} r_1 \\ r_2 \\ r_3 \\ r_4 \\ r_5 \end{pmatrix}$$

Hyperspherical coordinate transformation



← The “Jacobi Tree” used to define the hyperangular coordinates

And the squared hyperradius is defined by:

$$\tan \alpha_j = \frac{\sqrt{\sum_{k=1}^j \rho_k^2}}{\rho_{j+1}}$$

$$R^2 = \sum_{j=1}^{N_{\text{rel}}} \rho_j^2$$

This can be defined for any N-particle problem, and it is proportional to the trace of the moment of inertia tensor.

arXiv:1504.07884

Phys. Rev. B 92, 125427 (2015)

non-interacting relative Hamiltonian

In hyperspherical coordinates:

$$H_{\text{rel}} = -\frac{1}{2\mu} \nabla_{R,\Omega}^2 + \frac{\mu}{8} R^2 + \frac{1}{2\hbar} L_z^{\text{rel,tot}}$$

$$\nabla_{R,\Omega}^2 = \frac{1}{R^{2N_{\text{rel}}-1}} \partial_R R^{2N_{\text{rel}}-1} \partial_R - \frac{\hat{K}^2}{R^2}$$

\hat{K} is called the grand angular momentum operator

The eigenstates of \hat{K}^2 are the hyperspherical harmonics, $\Phi_{Ku}^{(M)}(\Omega)$, where

$$\hat{K}^2 \Phi_{Ku}^{(M)}(\Omega) = K(K + 2N_{\text{rel}} - 2) \Phi_{Ku}^{(M)}(\Omega)$$

The final quantum number K here is called the “grand angular momentum quantum number”, $K = |M|, |M|+2, |M|+4, \dots$

Now apply this adiabatic hyperspherical method to the quantum Hall problem

How to define the “filling factor”

$$\nu = \frac{\rho h}{eB} = \frac{N\phi_0}{BA}$$

$\phi_0 = h/e$ in S.I. units

$$\langle R^2 \rangle_{N,r_c} = \frac{(N-1)r_c^2}{2\mu}$$

fundamental flux quantum

Typical GaAs
e density: $\rho = 2.4 \times 10^{11} \text{ cm}^{-2}$

$$\nu = \frac{N(N-1)}{2K}$$

**=HYPERSPHERICAL
FILLING FACTOR**

the $\nu = 1$ quantum

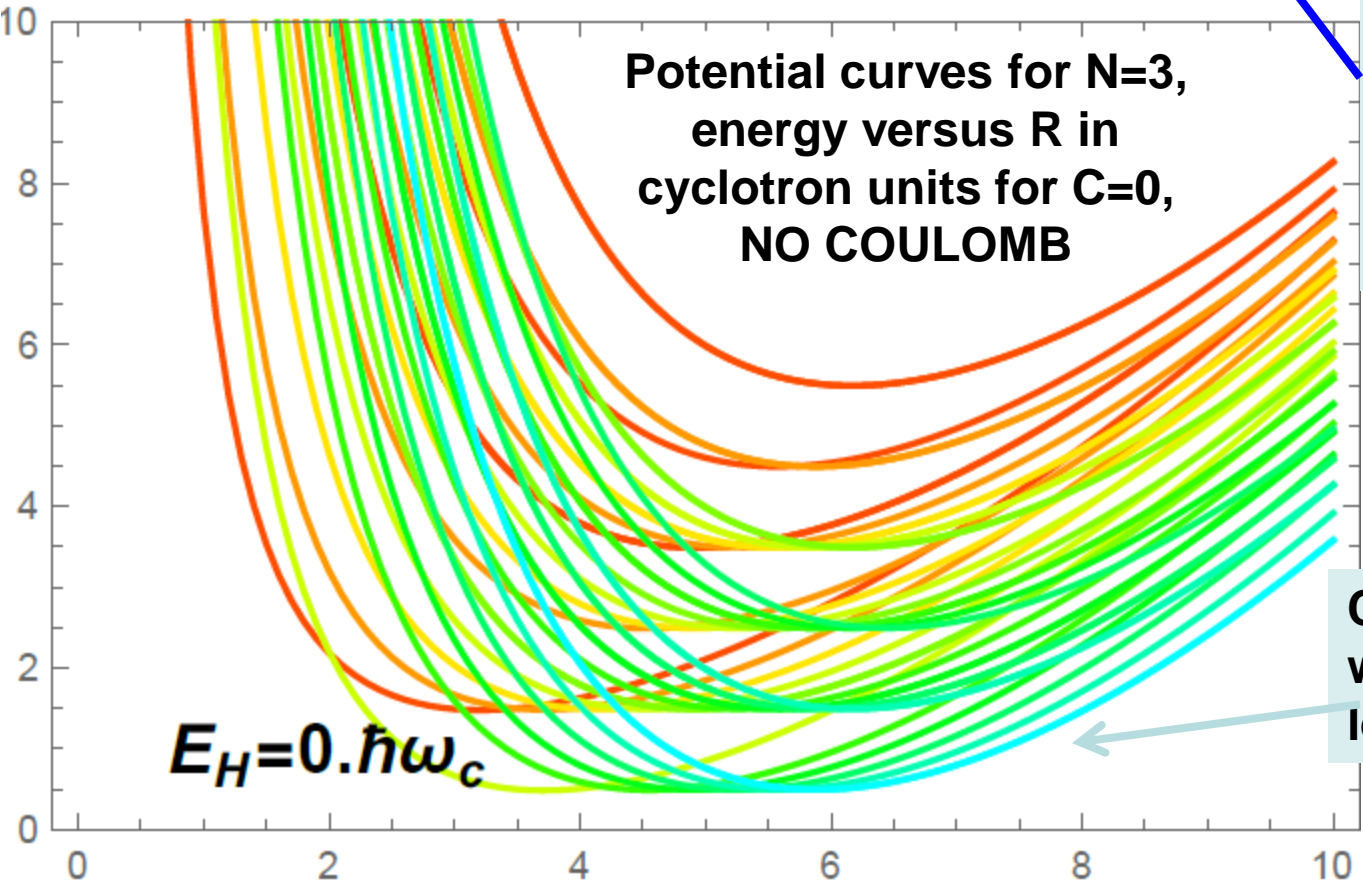
Hall state is found at a magnetic field near $B = 10\text{T}$ and the $\nu = 1/3$ state occurs around the much higher field $B \approx 29\text{T}$.

Potential energy curves for N noninteracting electrons in 2D in a B-field as a function of the hyperradius

$$U_{KM\gamma}(R) = \frac{(K + N - \frac{3}{2})(K + N - \frac{5}{2})}{2\mu R^2} + \kappa \frac{C_{KM\gamma}}{R} + \frac{1}{8}\mu R^2 + \frac{1}{2}M$$

Antisymmetrization has been carried out, and most curves shown are highly degenerate

This term vanishes if no Coulomb interactions. These C are eigenvalues of the Coulomb interaction within a degenerate K,M-space



$$\kappa = \frac{e^2}{4\pi\epsilon\lambda_0} \frac{1}{\hbar\omega_c}$$

Channels associated with the lowest Landau level, $K=-M=|M|$

R, hyperradius in cyclotron units

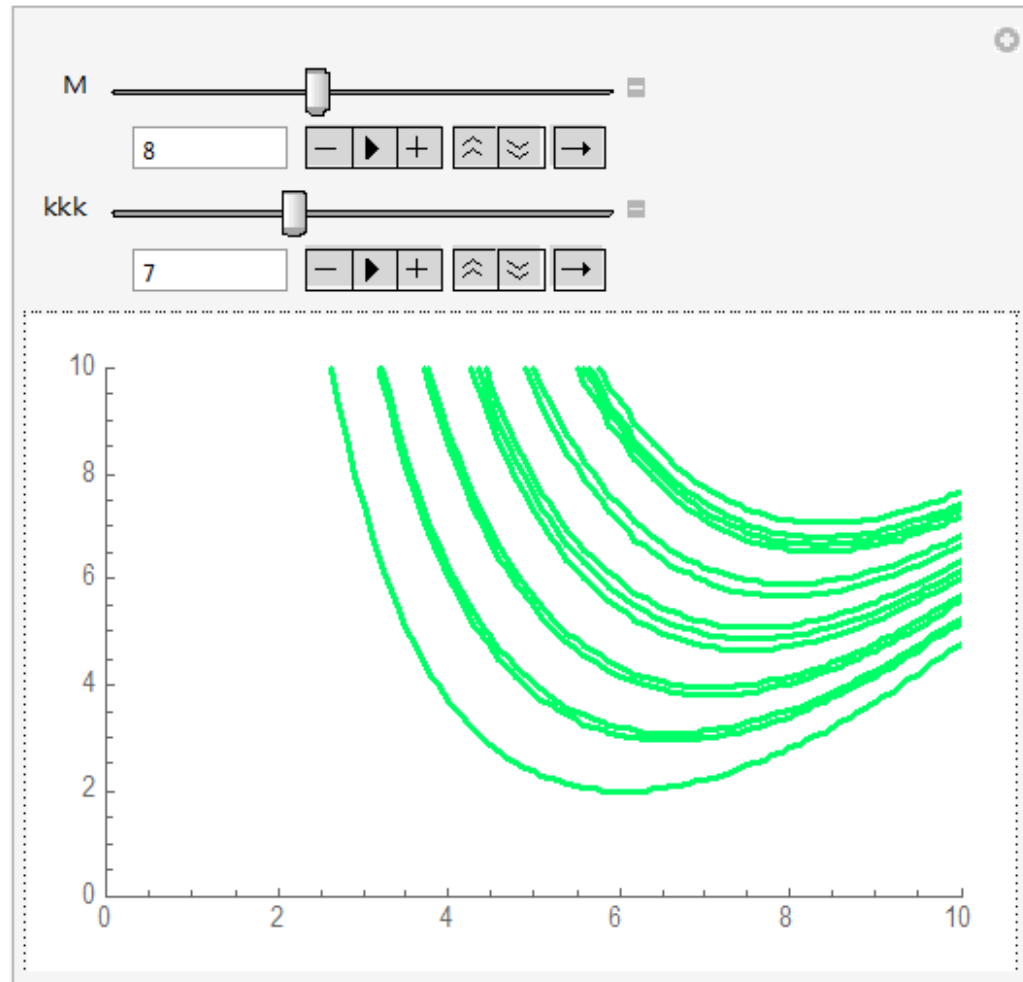
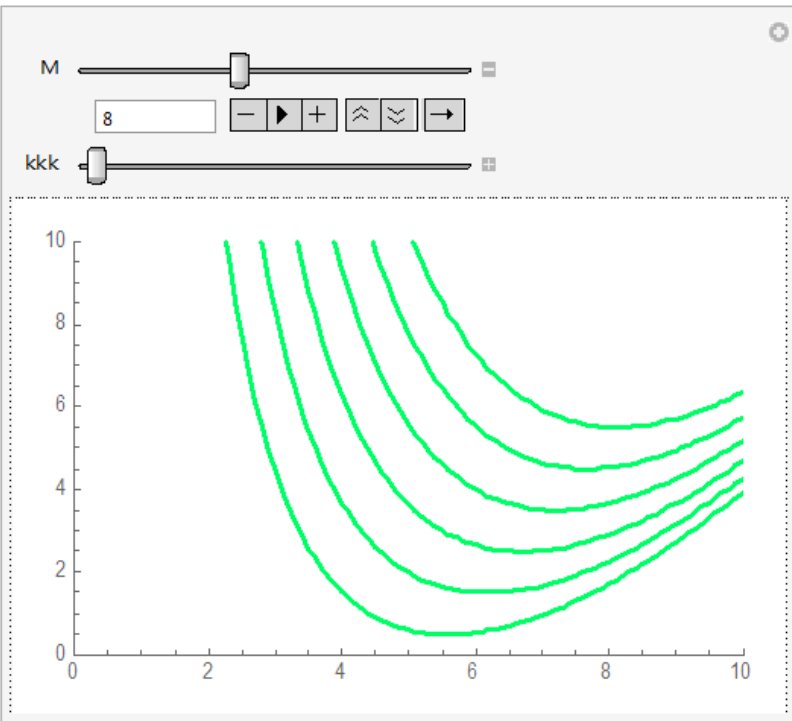
$K=-M=8$

3 particles

A non-FQHE state

With Coulomb interactions

noninteracting



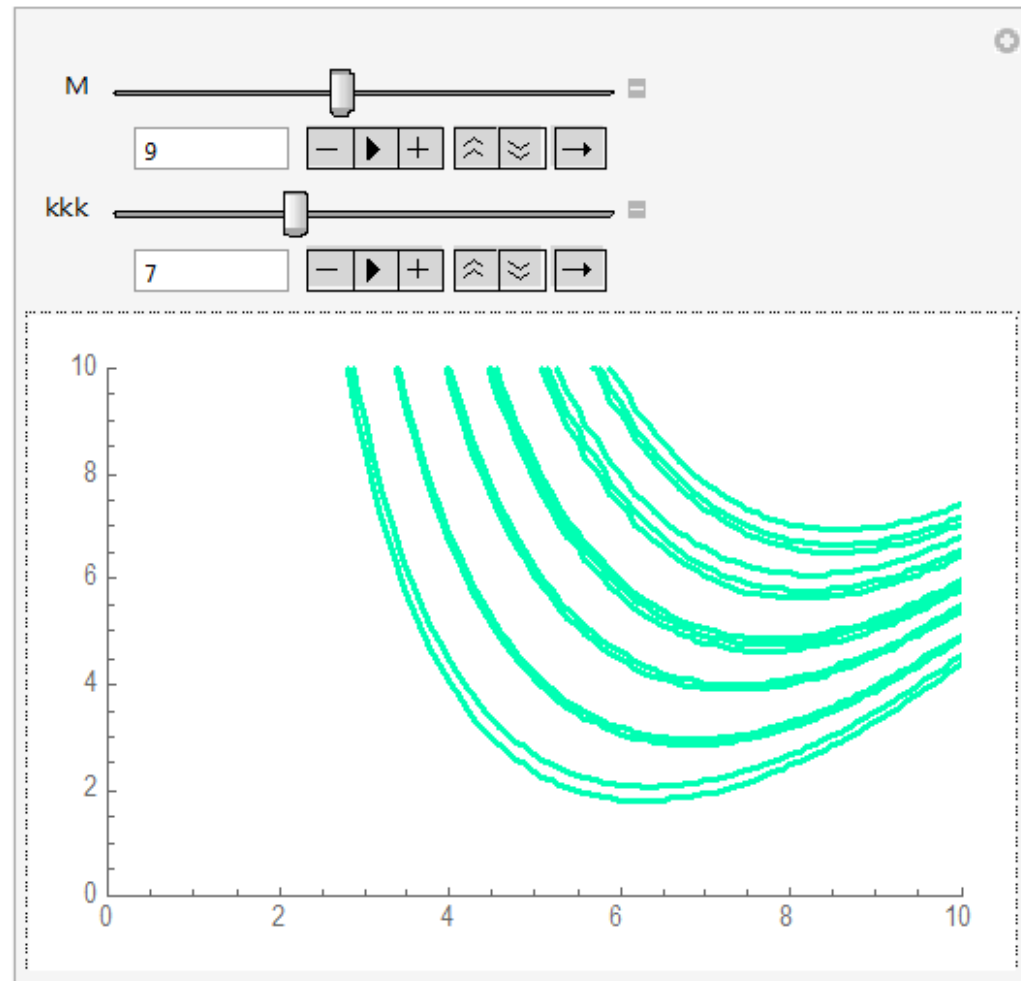
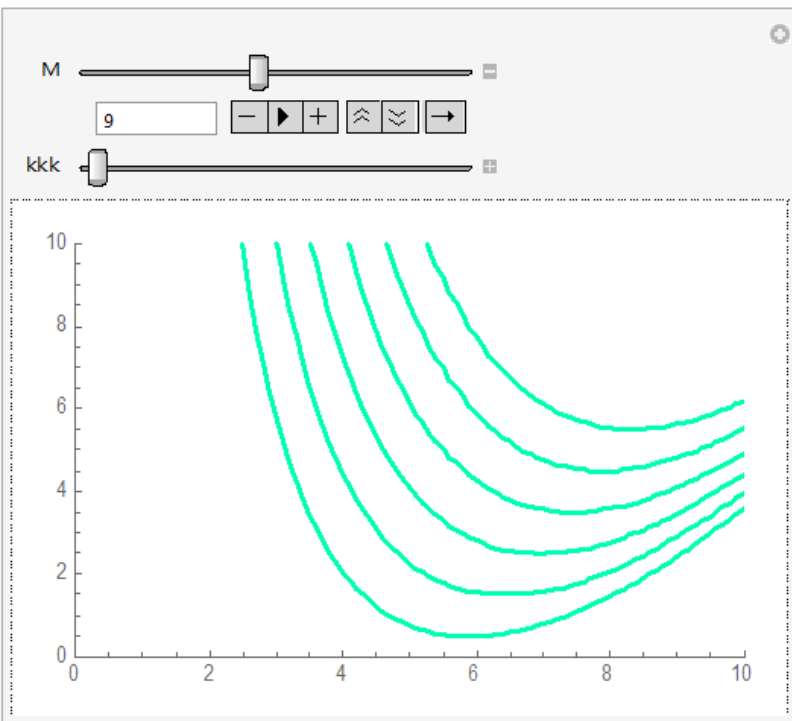
$$K=-M=9$$

3 particles

The Laughlin 1/3 state emerges for this symmetry, because the jump in degeneracy from 1 to 2 allows the system to minimize the Coulomb repulsion effectively

With Coulomb interactions

noninteracting



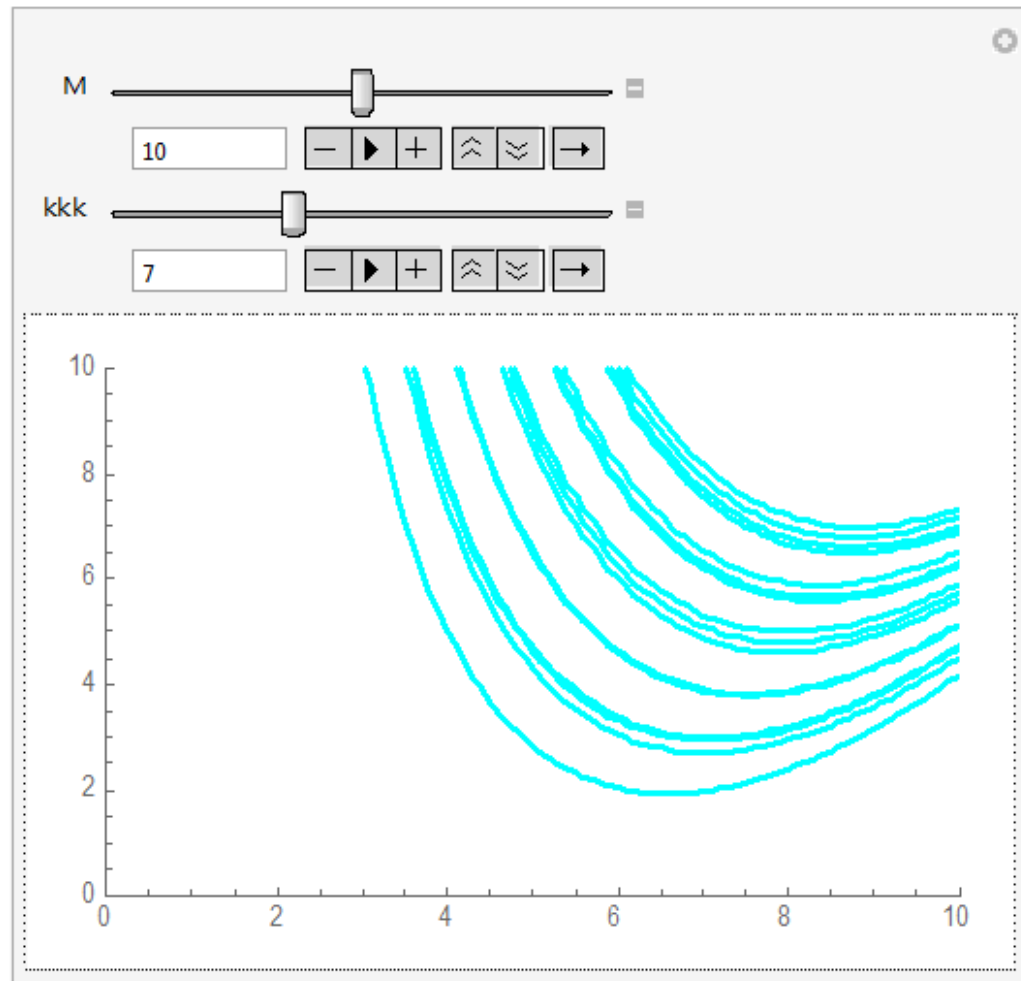
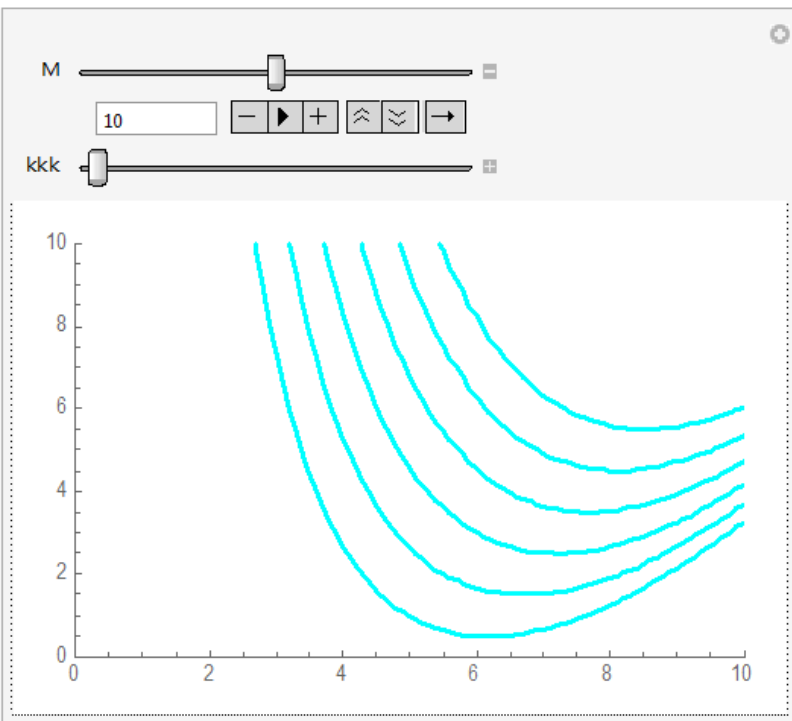
$K=-M=10$

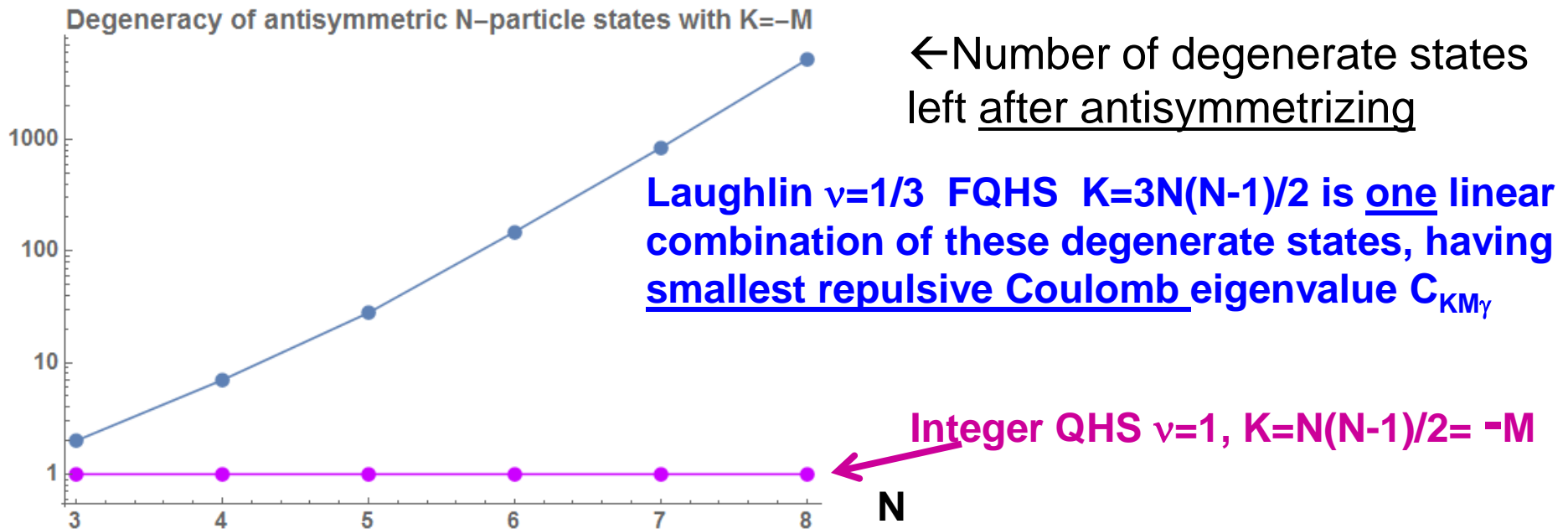
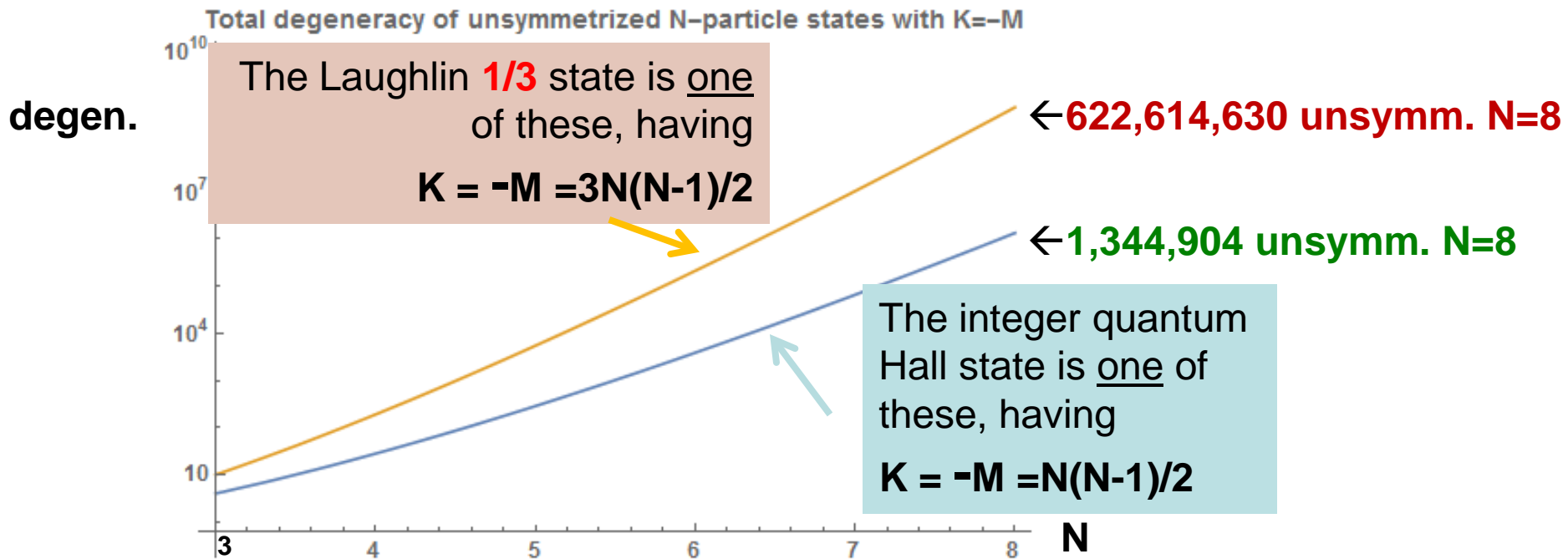
3 particles

A non-FQHE state

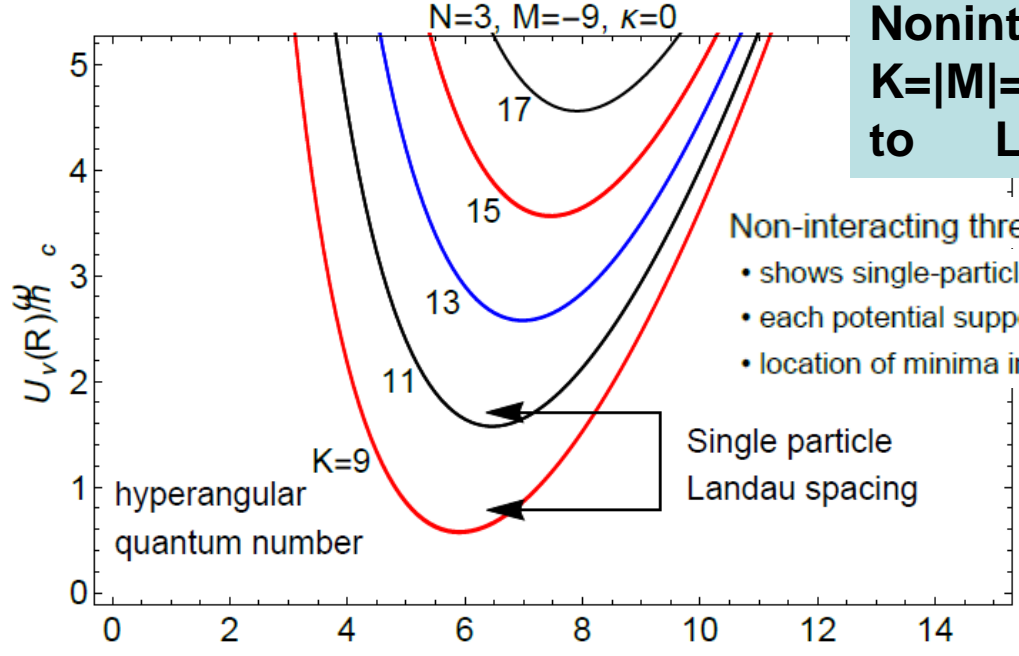
With Coulomb interactions

noninteracting

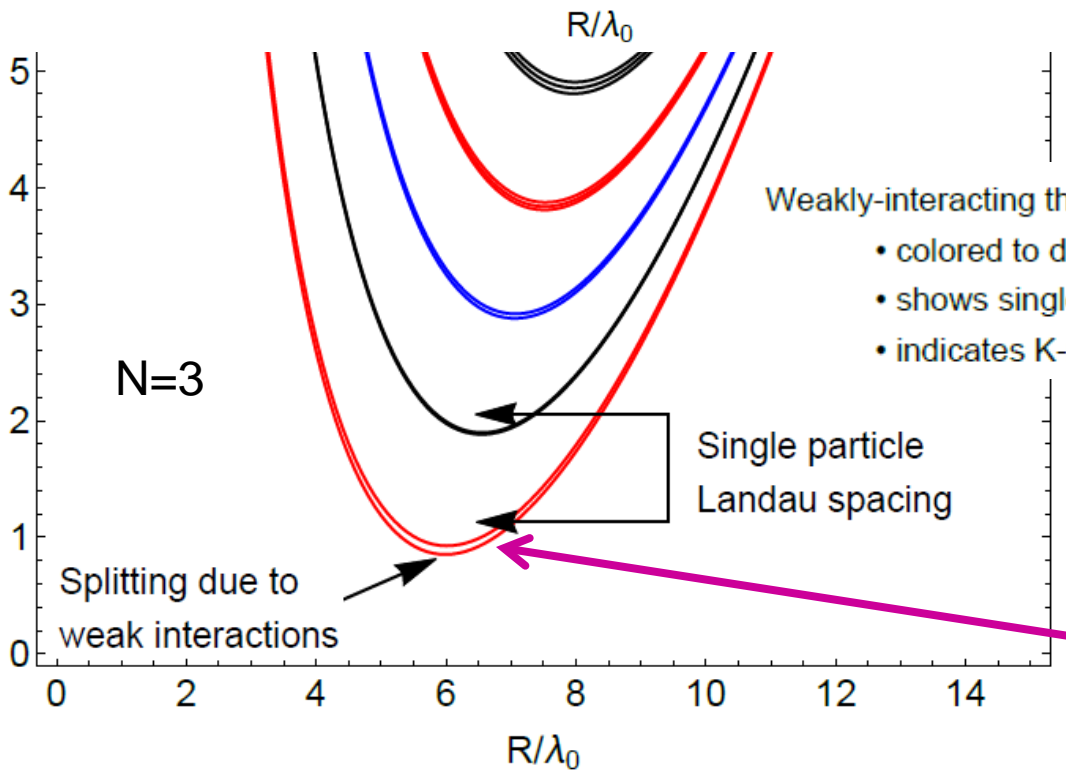
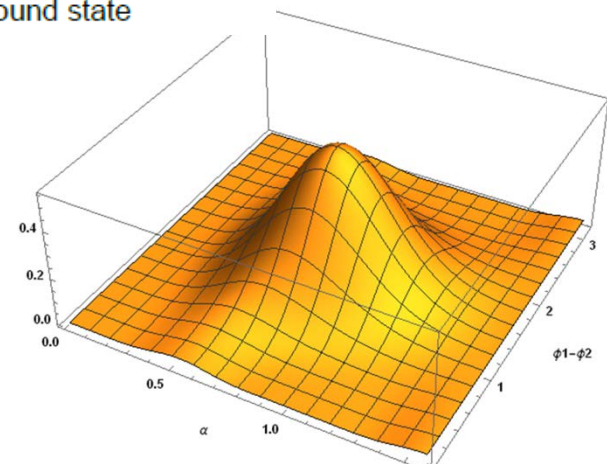




Noninteracting states for $K=|M|=9,11,13,15,\dots$, corresponding to $LL = 0, 1, 2, 3, \dots$ resp.



- Non-interacting three-body system in magnetic units.
- shows single-particle energy spacing
 - each potential supports an infinite number of bound states
 - location of minima indicate "size" of bound state



- Weakly-interacting three-body system in magnetic units.
- colored to distinguish different K -manifolds
 - shows single-particle energy spacing is larger than that of interactions
 - indicates K -manifolds are, in general, degenerate

The lower hyperangular wavefunction here has a 99% overlap with the 1/3 Laughlin wfn

Now look at some quantitative measures of accuracy for the hyperspherical method, compared with others:

Quantized motion of three two-dimensional electrons in a strong magnetic field

R. B. Laughlin

University of California, Lawrence Livermore National Laboratory, Livermore, California 94550

We have found a simple, exact solution of the Schrödinger equation for three two-dimensional electrons in a strong magnetic field, given the assumption that they lie in a single Landau level. We find that the interelectronic spacing has characteristic values, not dependent on the form of the interaction, which change discontinuously as pressure is applied, and that the system has characteristic excitation energies of approximately $0.03e^2/a_0$, where a_0 is the magnetic length.

3386

R. B. LAUGHLIN

27

TABLE I. Coulomb matrix elements across the states $|m, n\rangle$ defined by Eq. (18) in units of $(3/\sqrt{2})/(e^2/a_0)$. Quantum numbers m, n are indicated in parenthesis. $M=3m+2n$ is the total angular momentum. There are no states of $M=0, 1, 2$, or 4 .

$M=3$	(1,0)	$5.679\,0797 \times 10^{-1}$
$M=5$	(1,1)	$4.978\,3743 \times 10^{-1}$
$M=6$	(2,0)	$4.201\,1726 \times 10^{-1}$
$M=7$	(1,2)	$4.471\,2999 \times 10^{-1}$
$M=8$	(2,1)	$4.032\,3072 \times 10^{-1}$
$M=9$	(3,0)	$3.401\,7834 \times 10^{-1}$
	(1,3)	$1.306\,1401 \times 10^{-2}$

Next, Laughlin diagonalizes this matrix, i.e. applies degenerate perturbation theory in all coordinates

$1.306\,1401 \times 10^{-2}$
 $4.087\,2620 \times 10^{-1}$



TESTING ADIABATICITY

Comparison of energy level calculations in the adiabatic hyperspherical approximation with the Laughlin method (1983 Phys. Rev. B first row) which does degenerate perturbation theory in all degrees of freedom

	$N, -M$	3,9	3,15	4,18	5,30
1	ΔE , Perturbation Theory	0.716527	0.55248	1.30573	2.02725
2	ΔE , Degenerate fixed- K	0.704637	0.54792	1.28552	1.99742
3	ΔE , Born-Oppenheimer (lower bound*)	0.70198	0.54722	1.28086	1.99226
4	ΔE , Adiabatic (upper bound)	0.70204	0.54723	1.28092	1.99230

Row 1: degenerate perturbation theory in all coordinates (as in Laughlin, 1983, PRL; agrees with his numbers to all 8 digits; and Jain et al. 2006 arXiv for N=4,5)

Row 2: degenerate perturbation theory in the hyperangular degrees of freedom only, followed by exact solution in R

Row 3: full Born-Oppenheimer calculation, treating R adiabatically, giving lower bound (if converged) to the ground state energy

Row 4: full adiabatic approximation including repulsive “diagonal correction term” (d^2/dR^2), giving an upper bound to the ground state energy

Semiconductor quantum dots in high magnetic fields

The composite-fermion view

At our crudest level of approximation, we also find exact agreement with calculations by Jain et al.

Gun Sang Jeon^{1,2,a}, Chia-Chen Chang¹, and Jainendra K. Jain¹

Table 3. Comparison between the CF and the exact energies (V_{CF} and V_{ex}) for $N = 6$.

L	D	D^*	V_{ex}	V_{CF}	L	D	D^*	V_{ex}	V_{CF}	L	D	D^*	V_{ex}	V_{CF}	L	D	D^*	V_{ex}	V_{CF}
19	5	1	4.52568	4.52563(84)	52	2702	10	2.69635	2.70122(14)	85	38677	1	2.06506	2.06929(9)	118	216705	9	1.75766	1.76108(13)
20	7	1	4.39138	4.39214(47)	53	3009	5	2.66882	2.67239(64)	86	41134	5	2.06506	2.06911(12)	119	226479	3	1.74584	1.75185(20)
21	11	1	4.26439	4.26485(31)	54	3331	2	2.63071	2.63357(25)	87	43752	2	2.05433	2.05522(17)	120	236534	1	1.73124	1.73566(10)
22	14	3	4.26439	4.26557(67)	55	3692	1	2.58540	2.58872(13)	88	46461	9	2.04622	2.04944(24)	121	247010	3	1.73124	1.73575(13)
23	20	2	4.15579	4.15623(25)	56	4070	5	2.58541	2.58807(20)	89	49342	3	2.02791	2.03308(20)	122	257783	8	1.72727	1.73012(18)
24	26	1	4.05541	4.05721(58)	57	4494	2	2.55188	2.55252(31)	90	52327	1	2.00538	2.00952(20)	123	269005	2	1.72031	1.72323(11)
25	35	1	3.92152	3.92355(10)	58	4935	9	2.54880	2.55221(22)	91	55491	3	2.00538	2.00969(35)	124	280534	4	1.70935	1.71436(23)
26	44	3	3.90771	3.90868(73)	59	5427	3	2.51327	2.51647(68)	92	58767	8	1.99893	2.00142(44)	125	292534	1	1.69562	1.69987(6)
27	58	2	3.79370	3.79420(72)	60	5942	1	2.47124	2.47423(27)	93	62239	2	1.98517	1.98615(10)	126	304865	2	1.69562	1.69984(3)
28	71	5	3.79370	3.79447(29)	61	6510	3	2.47124	2.47420(61)	94	65827	4	1.97151	1.97625(13)	127	317683	5	1.69191	1.69581(16)
29	90	2	3.69049	3.69200(92)	62	7104	8	2.45835	2.45998(31)	95	69624	1	1.95061	1.95495(22)	128	330850	9	1.68552	1.68900(11)
30	110	1	3.56719	3.56824(40)	63	7760	2	2.42388	2.42431(35)	96	73551	2	1.95061	1.95514(20)	129	344534	1	1.67503	1.68120(11)
31	136	3	3.56264	3.56580(66)	64	8442	4	2.40947	2.41278(12)	97	77695	5	1.94470	1.94832(11)	130	358579	2	1.66210	1.66513(14)
32	163	7	3.52932	3.53013(84)	65	9192	1	2.37120	2.37547(20)	98	81979	9	1.93471	1.93824(39)	131	373165	4	1.66210	1.66519(27)
33	199	2	3.41858	3.41952(30)	66	9975	2	2.37120	2.37513(14)	99	86499	1	1.91890	1.92278(10)	132	388138	7	1.65863	1.66131(18)
34	235	4	3.40210	3.40435(61)	67	10829	5	2.35951	2.36237(52)	100	91164	2	1.90010	1.90348(12)	133	403670	12	1.65264	1.65522(33)
35	282	1	3.28942	3.29204(19)	68	11720	9	2.34182	2.34476(24)	101	96079	4	1.90010	1.90329(29)	134	419609	18	1.64273	1.64584(15)
36	331	2	3.28587	3.29094(28)	69	12692	1	2.30954	2.31154(17)	102	101155	7	1.89472	1.89762(22)	135	436140	1	1.63050	1.63876(7)
37	391	5	3.25902	3.26178(31)	70	13702	2	2.28245	2.28574(35)	103	106491	12	1.88550	1.88831(53)	136	453091	1	1.63050	1.63878(14)
38	454	9	3.21604	3.21752(83)	71	14800	4	2.28245	2.28624(68)	104	111999	18	1.87118	1.87361(51)	137	470660	2	1.62723	1.63454(7)
39	532	1	3.11031	3.11221(29)	72	15944	7	2.27239	2.27584(8)	105	117788	1	1.85328	1.86170(17)	138	488678	3	1.62159	1.62801(1)
40	612	2	3.06846	3.07277(56)	73	17180	12	2.25596	2.25924(17)	106	123755	1	1.85328	1.86180(13)	139	507334	4	1.61221	1.61833(7)
41	709	4	3.06846	3.07263(46)	74	18467	18	2.23266	2.23432(46)	107	130019	2	1.84828	1.85551(23)	140	526461	2	1.60064	1.60352(19)
42	811	7	3.03681	3.03929(84)	75	19858	1	2.20188	2.20932(19)	108	136479	3	1.83963	1.84614(12)	141	546261	1	1.60064	1.60808(6)
43	931	12	3.00162	3.00288(91)	76	21301	1	2.20188	2.20944(22)	109	143247	4	1.82642	1.83222(16)	142	566547	10	1.59756	1.60028(38)
44	1057	18	2.95620	2.95640(61)	77	22856	2	2.19230	2.19868(34)	110	150224	2	1.80978	1.81276(9)	143	587535	5	1.59225	1.59806(30)
45	1206	1	2.86015	2.86444(21)	78	24473	3	2.17671	2.18392(17)	111	157532	1	1.80978	1.81507(10)	144	609040	2	1.58332	1.58980(9)
46	1360	1	2.86015	2.86427(33)	79	26207	4	2.15698	2.16067(26)	112	165056	10	1.80521	1.80836(23)	145	631269	1	1.57236	1.57642(6)

45 1206 1 2.86015 2.86444

Semiconductor quantum dots in high magnetic fields

The composite-fermion view

Gun Sang Jeon^{1,2,a}, Chia-Chen Chang¹, and Jainendra K. Jain¹

Eur. Phys. J. B 55, 271–282 (2007)

DOI: 10.1140/epjb/e2007-00060-4

From numerical “exact” calculations, the states that stand out as having lower energies than their neighboring M states are the Laughlin-type ($1/n$) and Jain-type states (primarily).

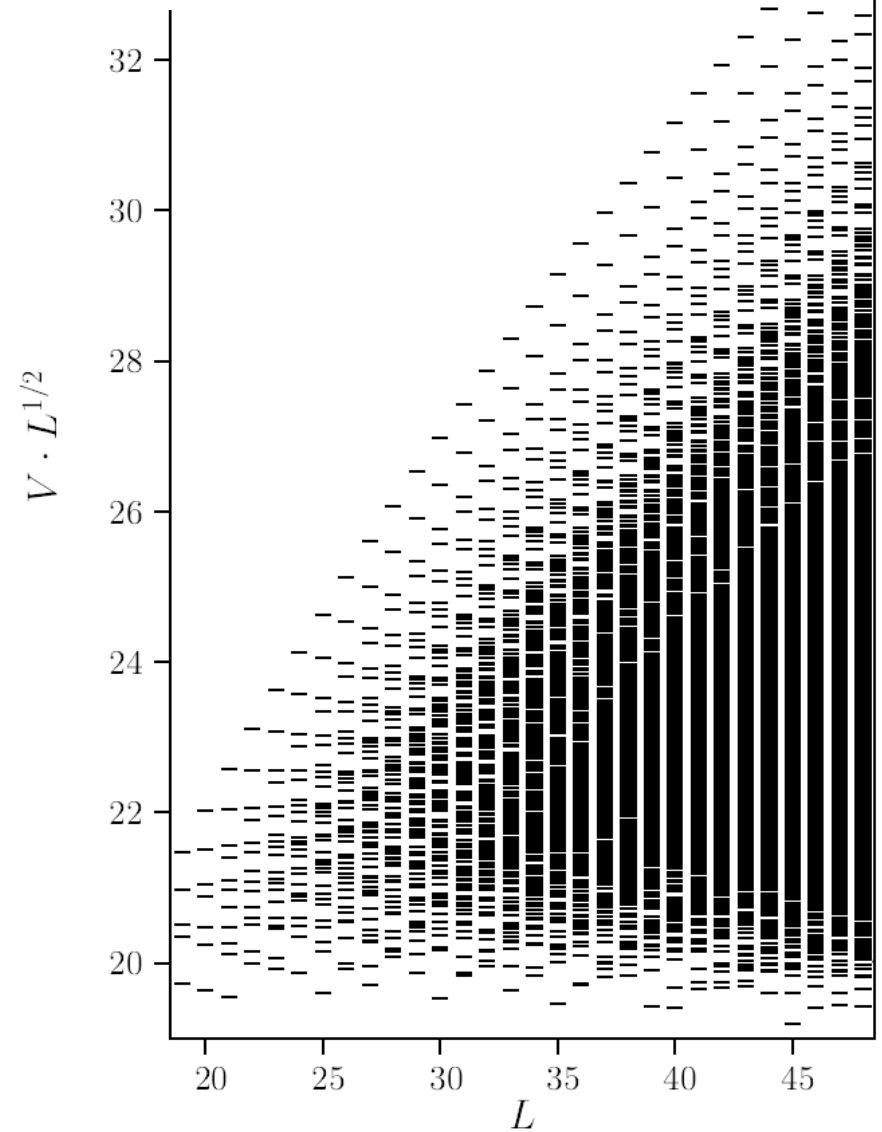


Fig. 6. Exact energy spectrum for $N = 6$.

Filling factor, $\nu \rightarrow$ 1/3 1/5 1/3 1/3 1/3

$N, -M$	3,9	3,15	4,18	5,30	6,45
ΔE , Haldane sphere, fit, extrapolation	0.71656	0.5526	1.310	2.04	≈ 3
ΔE , Planar calculations [47, 48]	0.716527	0.55248	1.30573	2.02725	2.86015
ΔE , Perturbation Theory	0.716527	0.55248	1.30573	2.02725	2.86015
ΔE , Degenerate fixed- K	0.704637	0.54792	1.28552	1.99742	2.81994
ΔE , Born-Oppenheimer (lower bound*)	0.70198	0.54722	1.28086	1.99226*	–
ΔE , Adiabatic (upper bound)	0.70204	0.54723	1.28092	1.99230	–

Energy level calculations in our hyperspherical coordinate picture, compared with previous calculations of quantum Hall effect pioneers Laughlin (1983 PRB) and from Jeong, Chang, & Jain (European Phys. J B 2007)

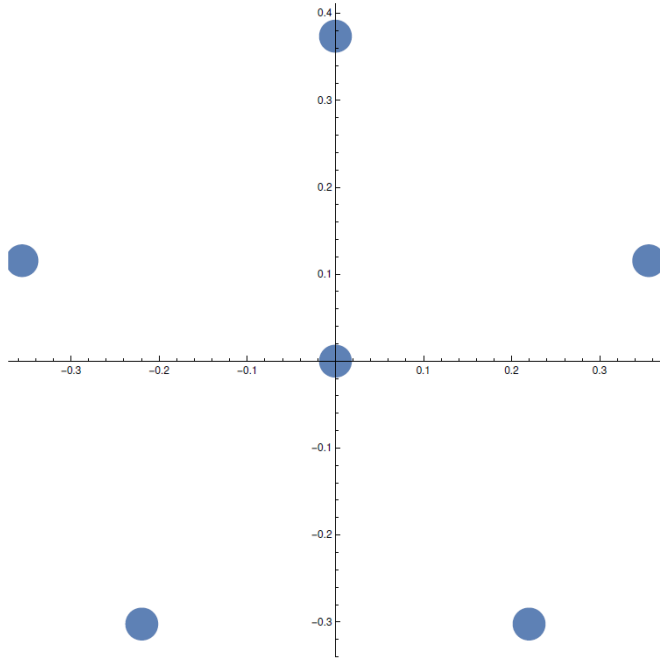
The lower bound calculations neglect the diagonal adiabatic correction term, which as shown by Starace and Webster (PRA 1979) must bound each exact energy level from below.

The upper bound calculations conform to the usual Rayleigh-Ritz variational principle and are guaranteed to give energies higher than or equal to the exact energy levels.

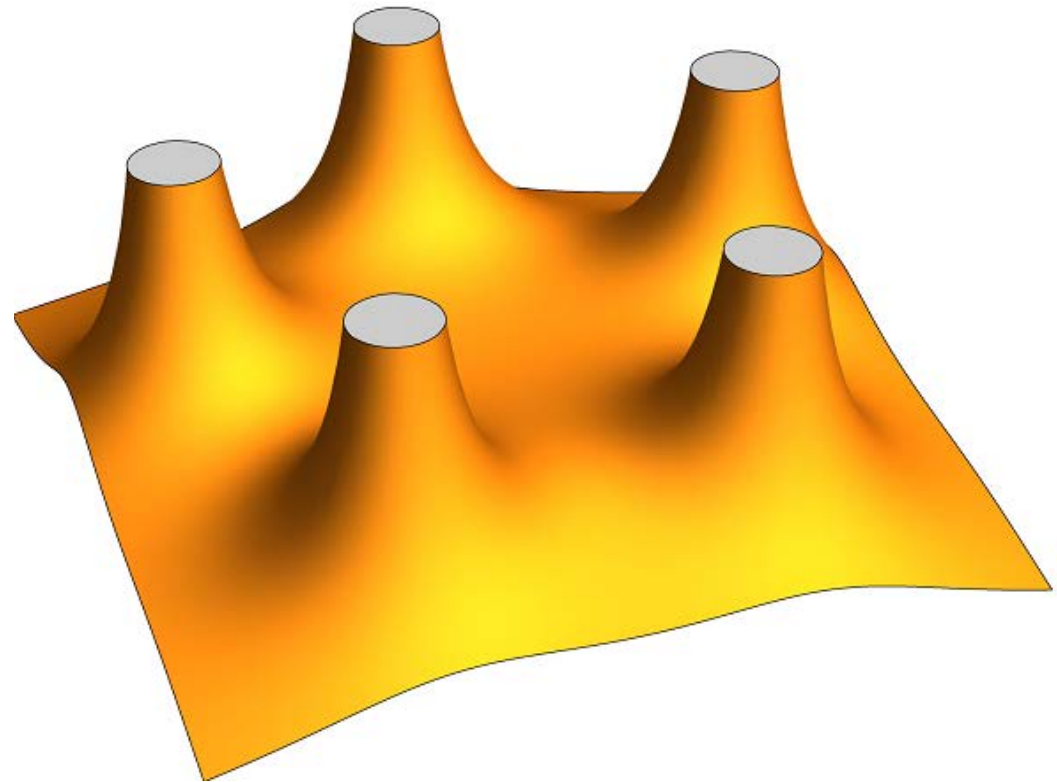
Finding: Our UPPER and LOWER bounds to the energy differ at around the 10⁻⁵ level. (In an AMO problem, the H- ground state, the difference is 1.9%). This indicates that quasi-separability in the hyperradial coordinate is VERY good.

Potential energy landscape at fixed hyperradius for 6 particles, in a configuration that minimizes the classical potential energy (left)

After minimization, this (right) figure shows the potential energy as the 6th particle is allowed to move throughout the plane at fixed R



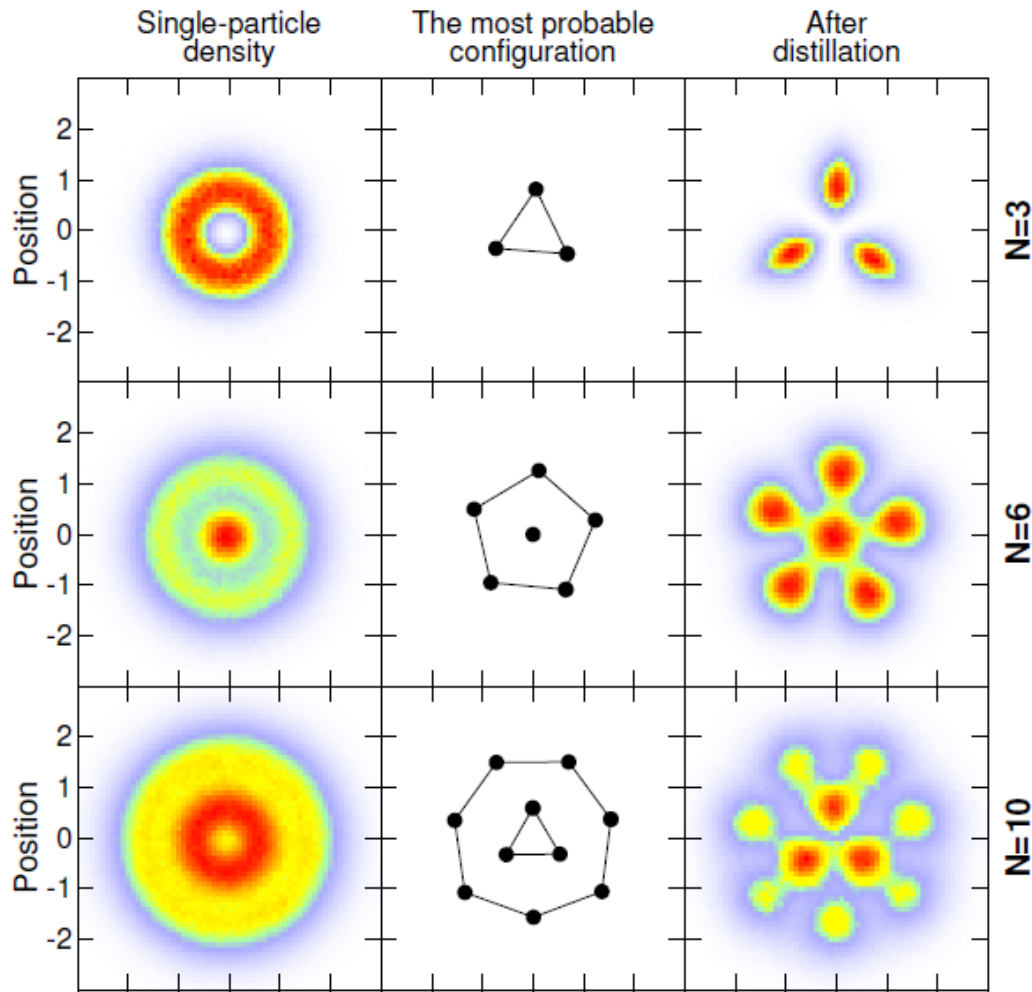
Minimum potential energy configuration



Potential energy landscape seen by the central electron

Pauli Crystals: hidden geometric structures of the quantum statistics

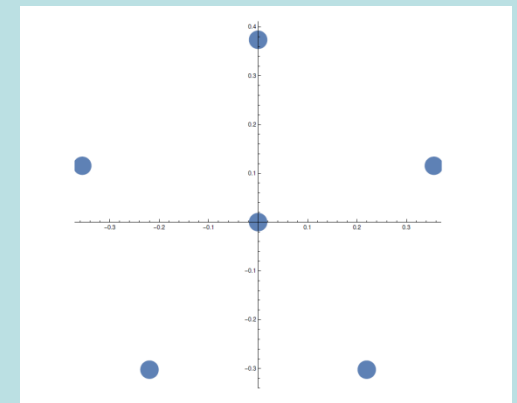
arXiv:1511.01036v2

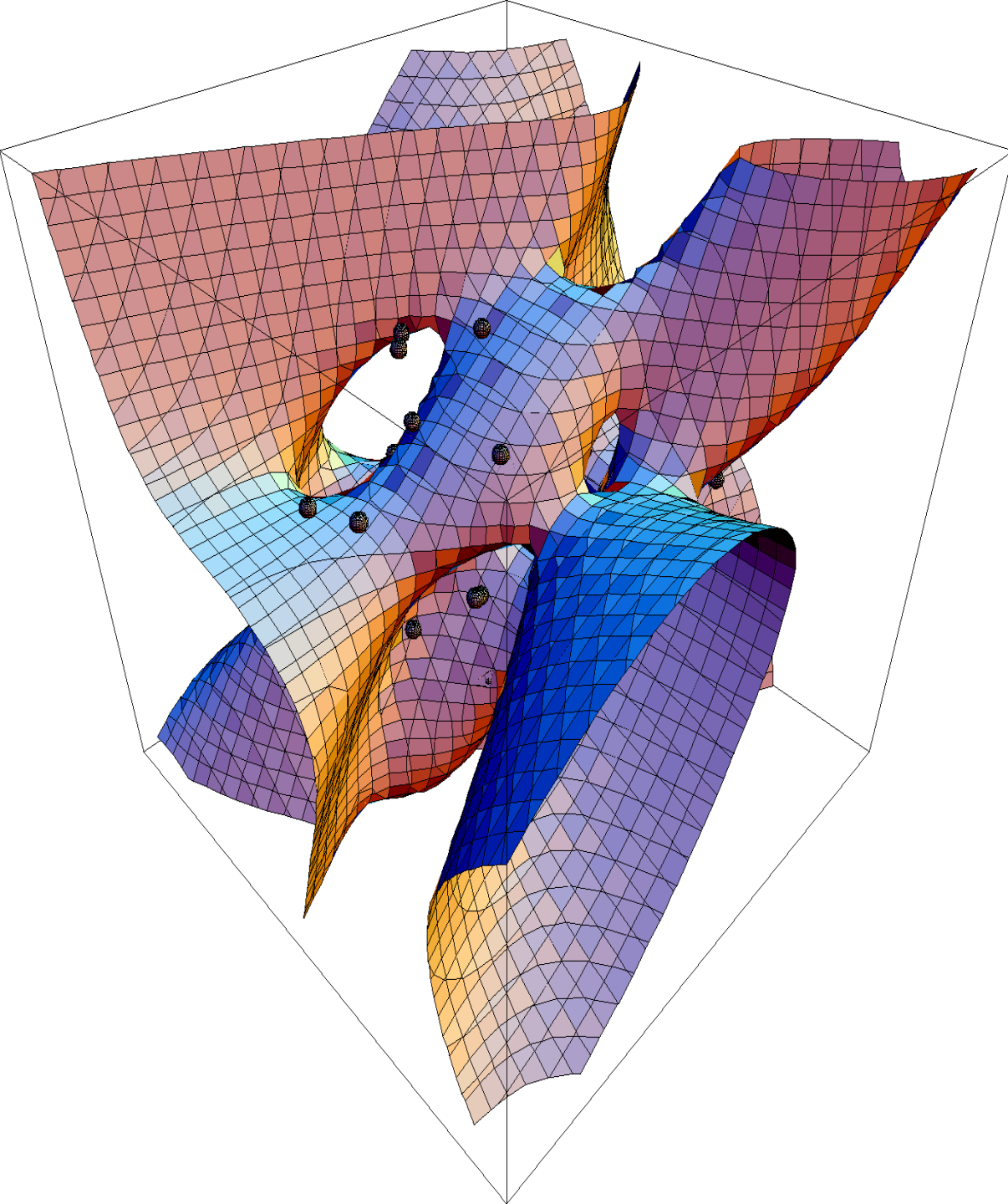


Noninteracting Quantum fermions



Coulomb-repelling classical fermions that minimize the repulsion at fixed hyperradius (present study)

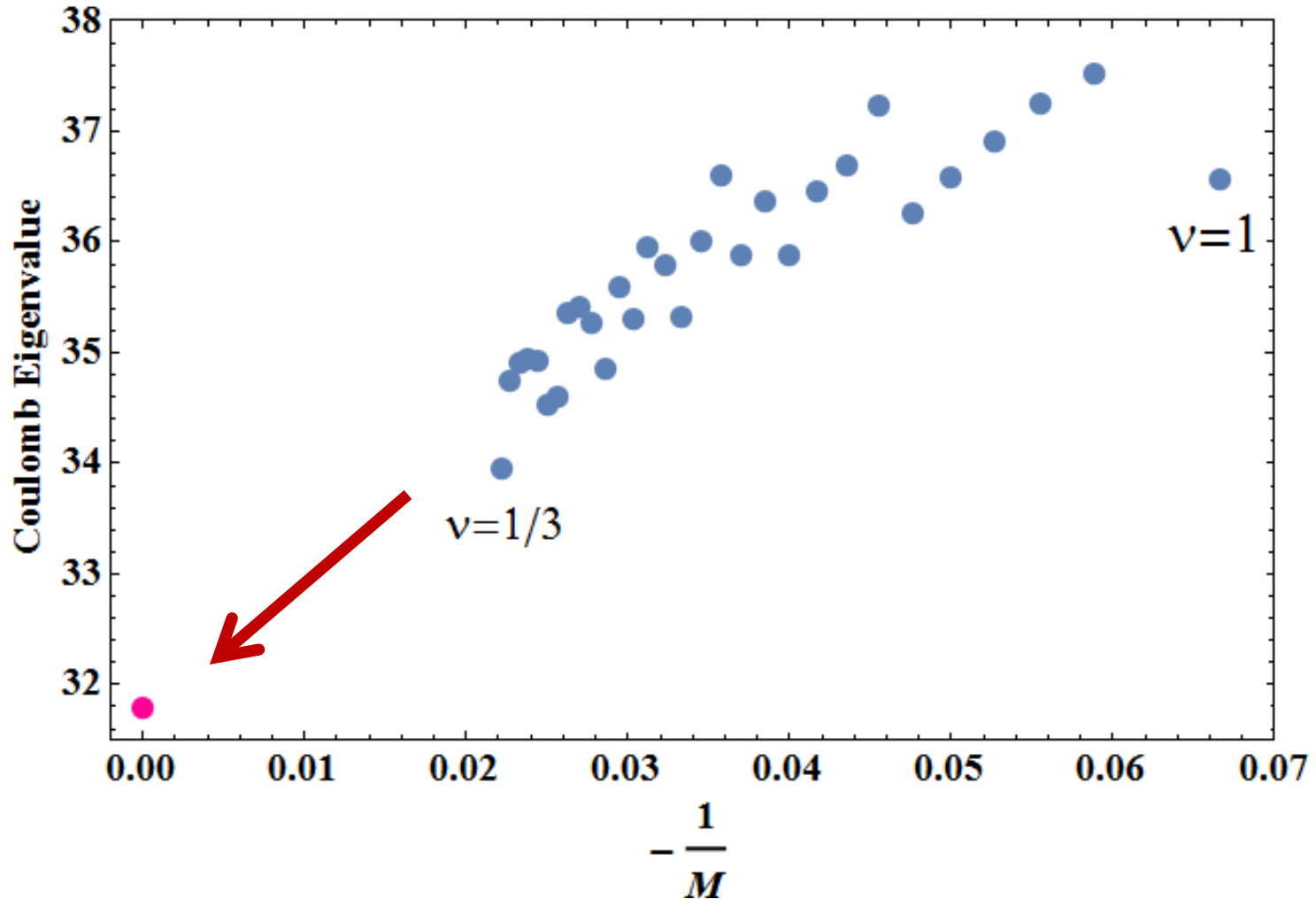




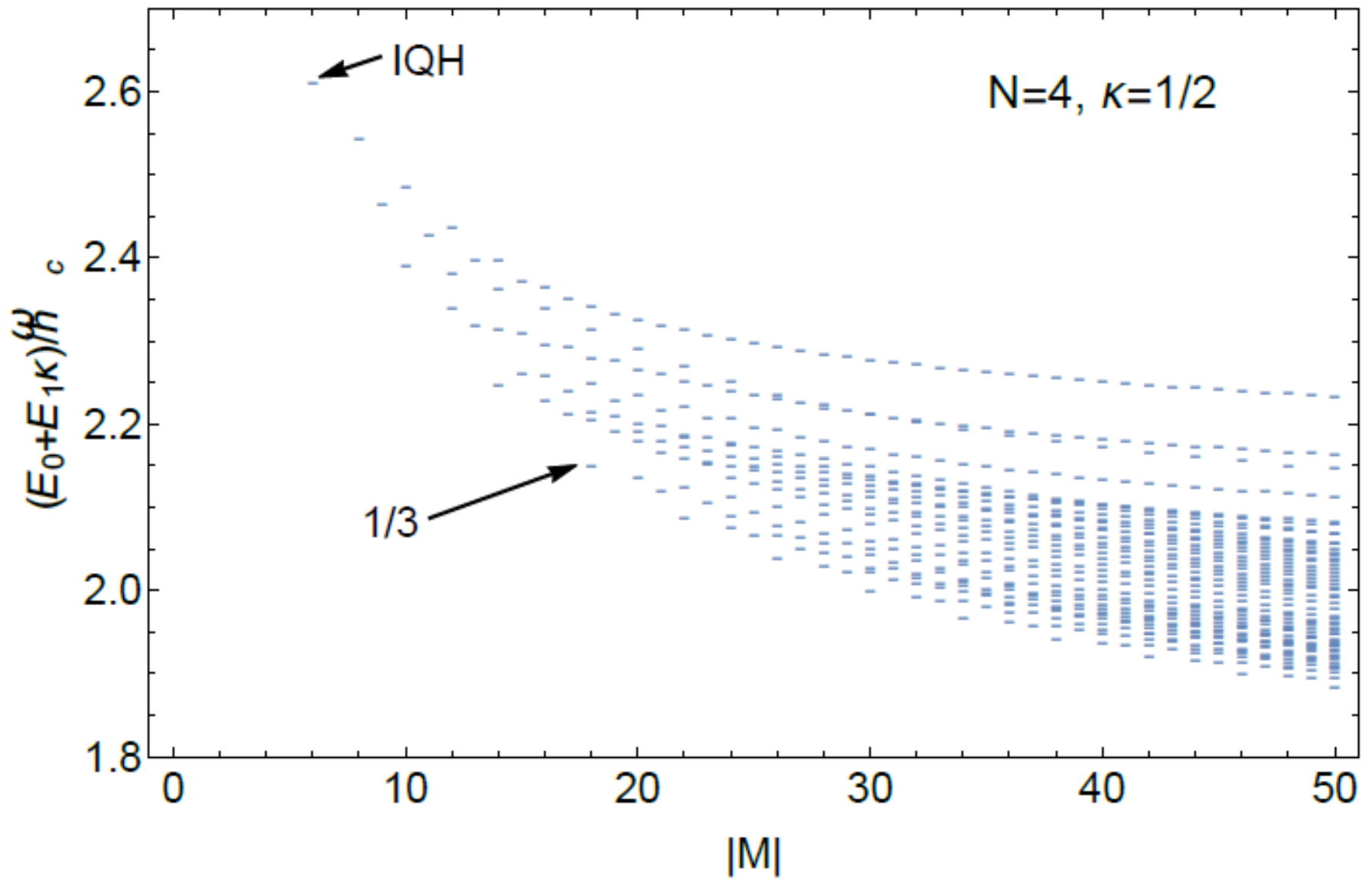
How does fixed-node Monte Carlo work for fermions? Take the nodal structure from a Slater determinant, and then let particles walk randomly and diffuse.

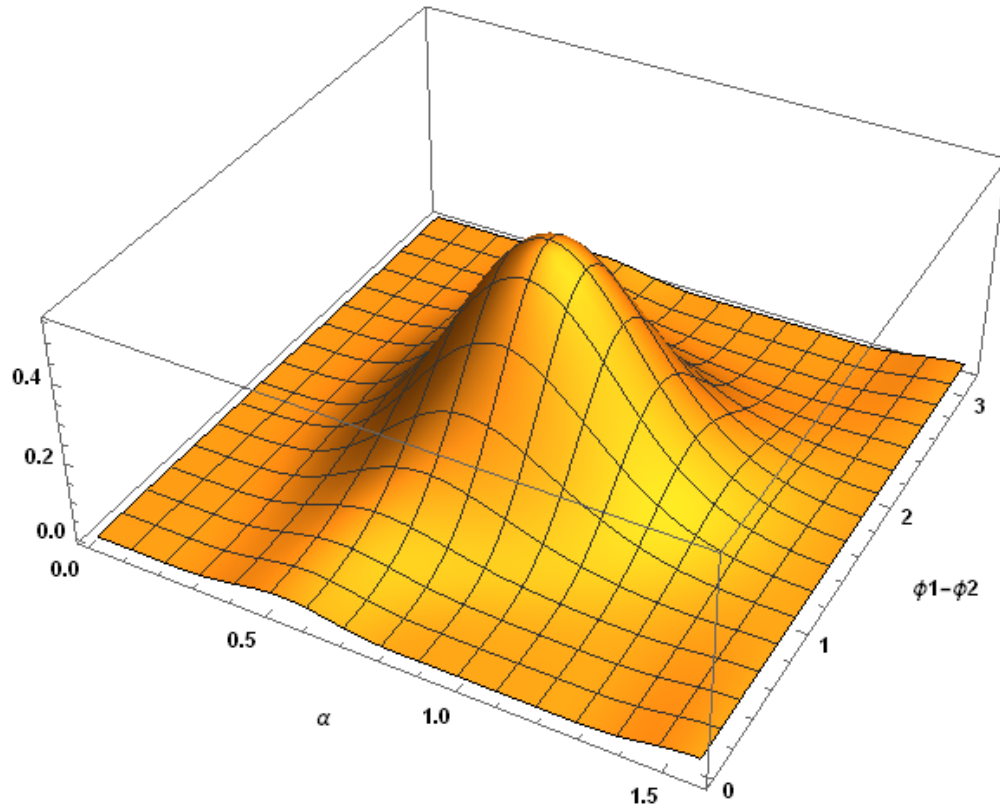
This graph shows the nodal structure of one particle, in a 56-particle spin-polarized DFG, with the positions of 55 particles chosen randomly and shown as small spheres.

Minimum quantum Coulomb potential eigenvalues for lowest $K=|M|$ (lowest Landau level) for 6 particles, showing their trend towards the classical minimum potential energy (magenta point) as K increases



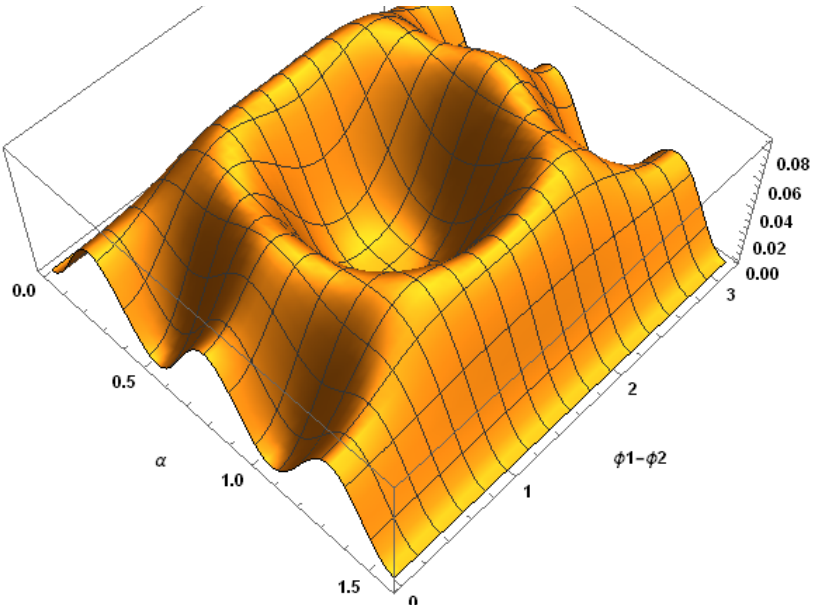
Eigenenergies for 4 particles after quantizing also in the hyperradius R





$K = -M = 9$ for $N = 3$

This $1/3$ Laughlin eigenstate has a strong **peak** at an equilateral triangle configuration, where electrons can stay as far apart as possible, minimize repulsion



$K = -M = 10$ for $N = 3$

This non-FQHE eigenstate has a deep **minimum** at an equilateral triangle configuration

**Next: an exploration of the role of DEGENERACY
within each $\{K,M\}$ manifold, and a conjecture**

Expectation: If there are more degenerate states, then the system has more degrees of freedom to minimize the Coulomb repulsion, and one expects that states of unusually low energy (like the Laughlin states $1/3$, $1/5$, etc....) will also have unusually high degeneracy compared to their neighbors.

Antisymmetrization of more than 5 or 6 particles is very challenging, and even learning how to count degeneracies is complicated, but one useful paper we found is:

S. H. Simon, E. H. Rezayi, and N. R. Cooper, [Phys. Rev. B **75**, 195306 \(2007\)](#).

Extending their treatment somewhat, we find a generating function can be used to compute the number of antisymmetric states $a_{|M|}^{(N)}$ for given $N, |M|$:

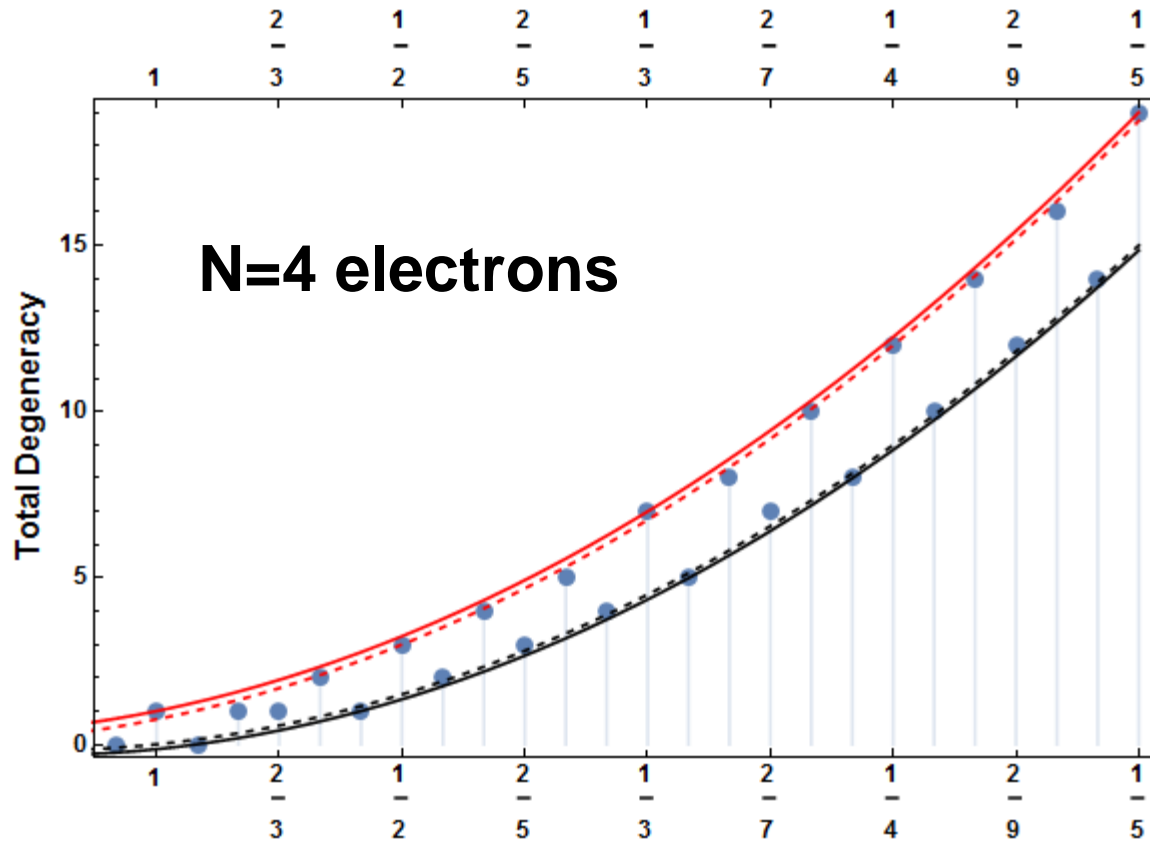
$$G_N(x) = x^{N(N-1)/2} \prod_{j=2}^N \frac{1}{1-x^j} = \sum_{|M|=0}^{\infty} a_{|M|}^{(N)} x^{|M|}.$$

Hint: use
Mathematica!

e.g. the Laughlin $1/3$ state for 12 particles occurs for **$M=-188$** ,
and the degeneracy of that manifold is: **$a_{|M|}^{(N)} = 5,929,008$**

On the role of exceptional degeneracy: e.g., from group theory, the number of antisymmetric states for **4 particles** in states with $K=|M|$ turns out to be the following:

$$\frac{|M|^2}{48} + \frac{1}{16} \left((-1)^{|M|} - 1 \right) |M| + \frac{1}{288} \left(64 \cos\left(\frac{2\pi|M|}{3}\right) - 9(-1)^{|M|} \left(4 \sin\left(\frac{\pi|M|}{2}\right) + 4 \cos\left(\frac{\pi|M|}{2}\right) + 3 \right) - 1 \right)$$



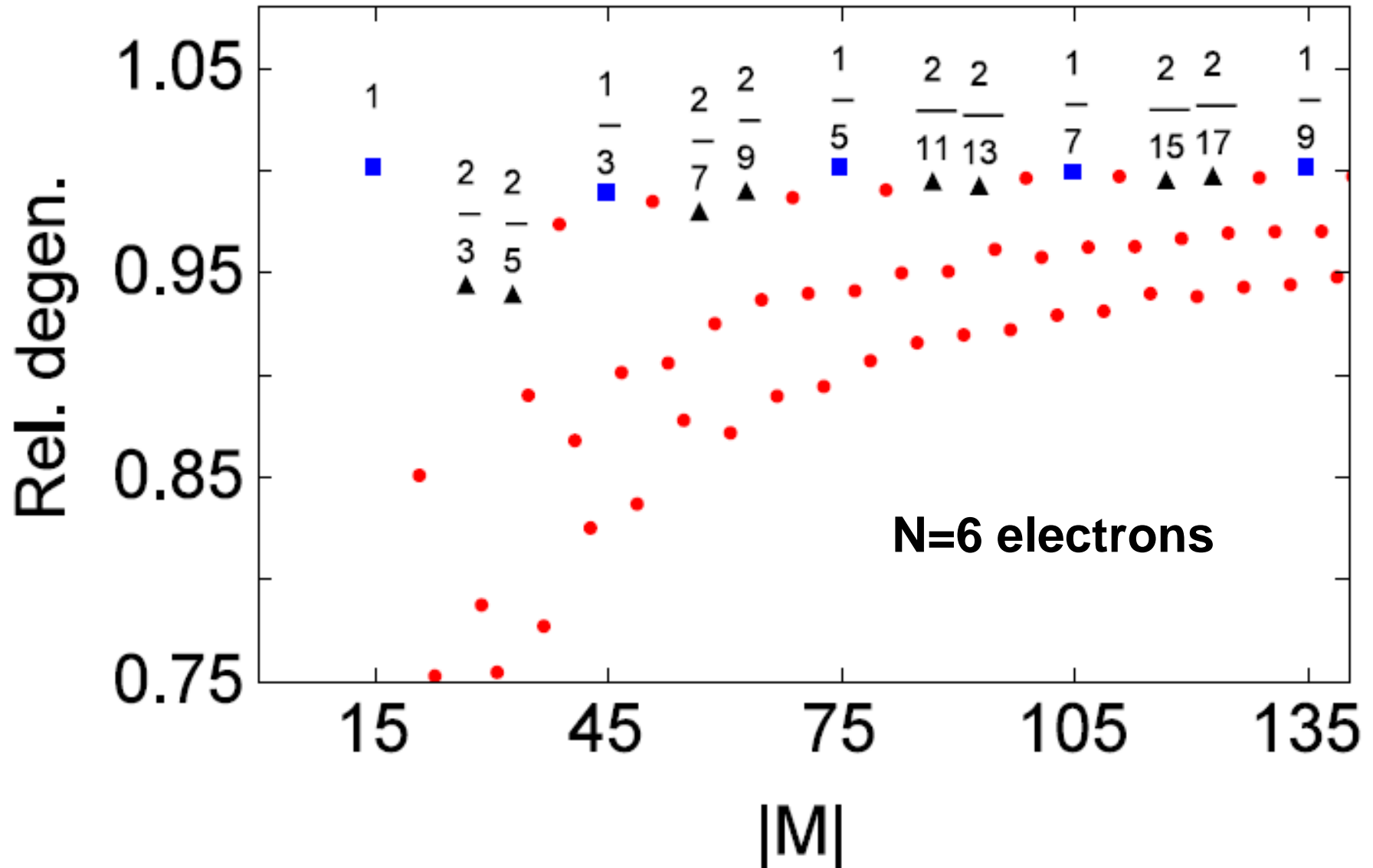
Note: the “hyperspherical filling factor”, which agrees with the usual definition for integer QHE and the Laughlin FQHE states, is given by

$$\nu^{hyp} = \frac{N(N-1)}{2K}$$

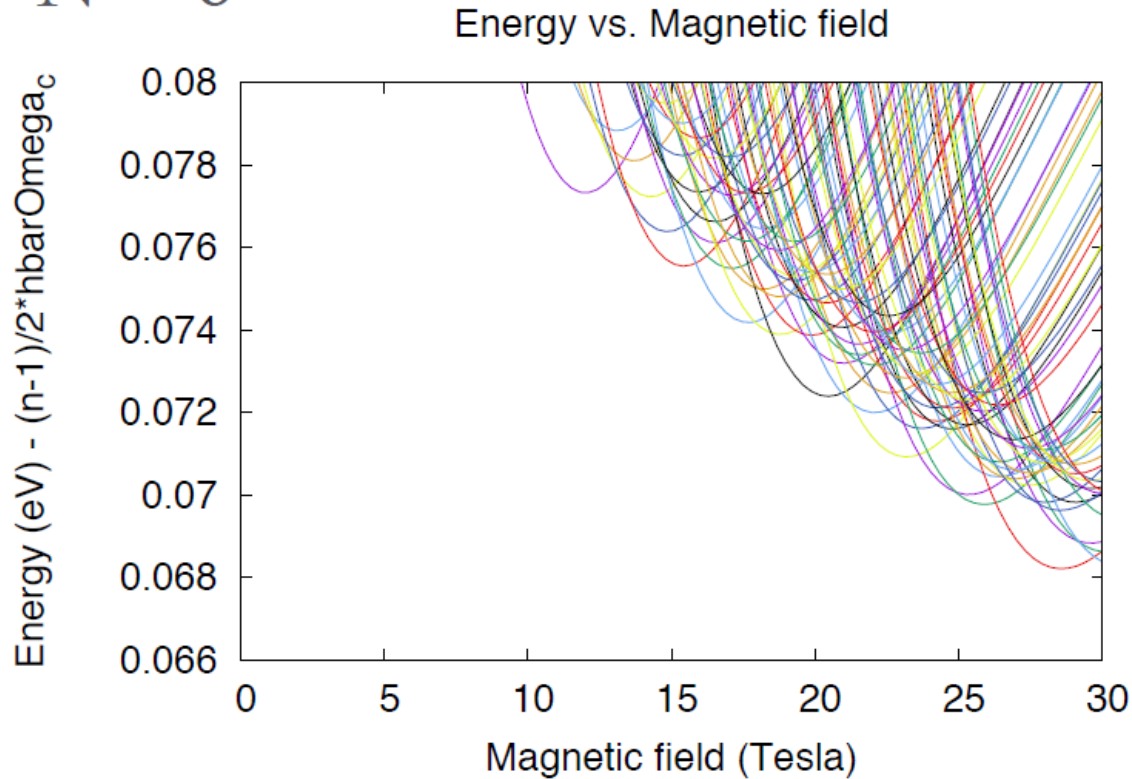
ν^{hyp}

Increasing $|M|=K$ = angular momentum \rightarrow

Connection between the high relative degeneracy states having known filling factors seen experimentally and in theory (Laughlin, Jain, etc.)



$N = 6$



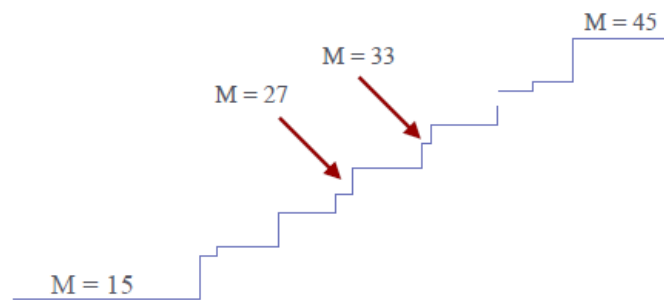
Lowest energy states:

$M = 15, 20, 21, 25, 27, 30, 33, 35, 39, 40, 45$

Important CF states:

$M = 15 \rightarrow \nu = 1;$
 $M = 27 \rightarrow \nu = 2/3$
 $M = 33 \rightarrow \nu = 2/5;$
 $M = 45 \rightarrow \nu = 1/3$

Devil's staircase:



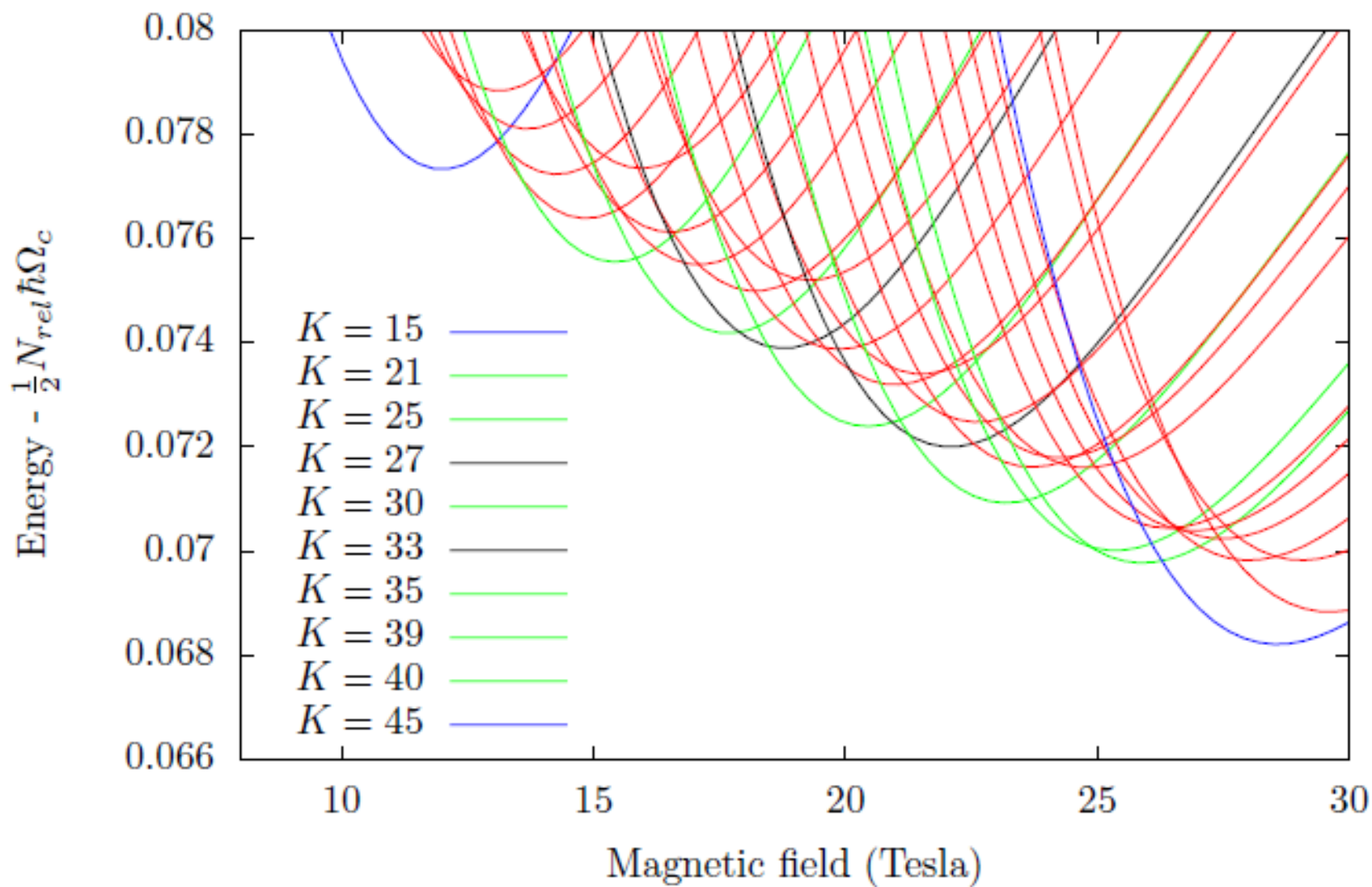
High degeneracy:
 $M = 15, 45, 39, 27, 33$
(all with relative degeneracy > 0.90)

N	$-M$	ν_{CF}	ν_{HS}	$(\frac{1}{\nu_{CF}} - \frac{1}{\nu_{HS}})$
3	3	1	1	0
	9	$\frac{1}{3}$	$\frac{1}{3}$	0
	15	$\frac{1}{5}$	$\frac{1}{5}$	0
4	6	1	1	0
	12	$\frac{2}{5}$	$\frac{1}{2}$	$-\frac{1}{2}$
	18	$\frac{1}{3}$	$\frac{1}{3}$	0
	24	$\frac{2}{7}$	$\frac{1}{4}$	$-\frac{1}{2}$
	30	$\frac{1}{5}$	$\frac{1}{5}$	0
6	15	1	1	0
	27	$\frac{2}{3}$	$\frac{5}{9}$	$-\frac{3}{10}$
	33	$\frac{2}{5}$	$\frac{5}{11}$	$\frac{3}{10}$
	45	$\frac{1}{3}$	$\frac{1}{3}$	0
	57	$\frac{2}{7}$	$\frac{5}{19}$	$-\frac{3}{10}$
	75	$\frac{1}{5}$	$\frac{1}{5}$	0

Connections between hyperspherical and conventional filling factors for known FQHE states for 3,4, and 6 electrons

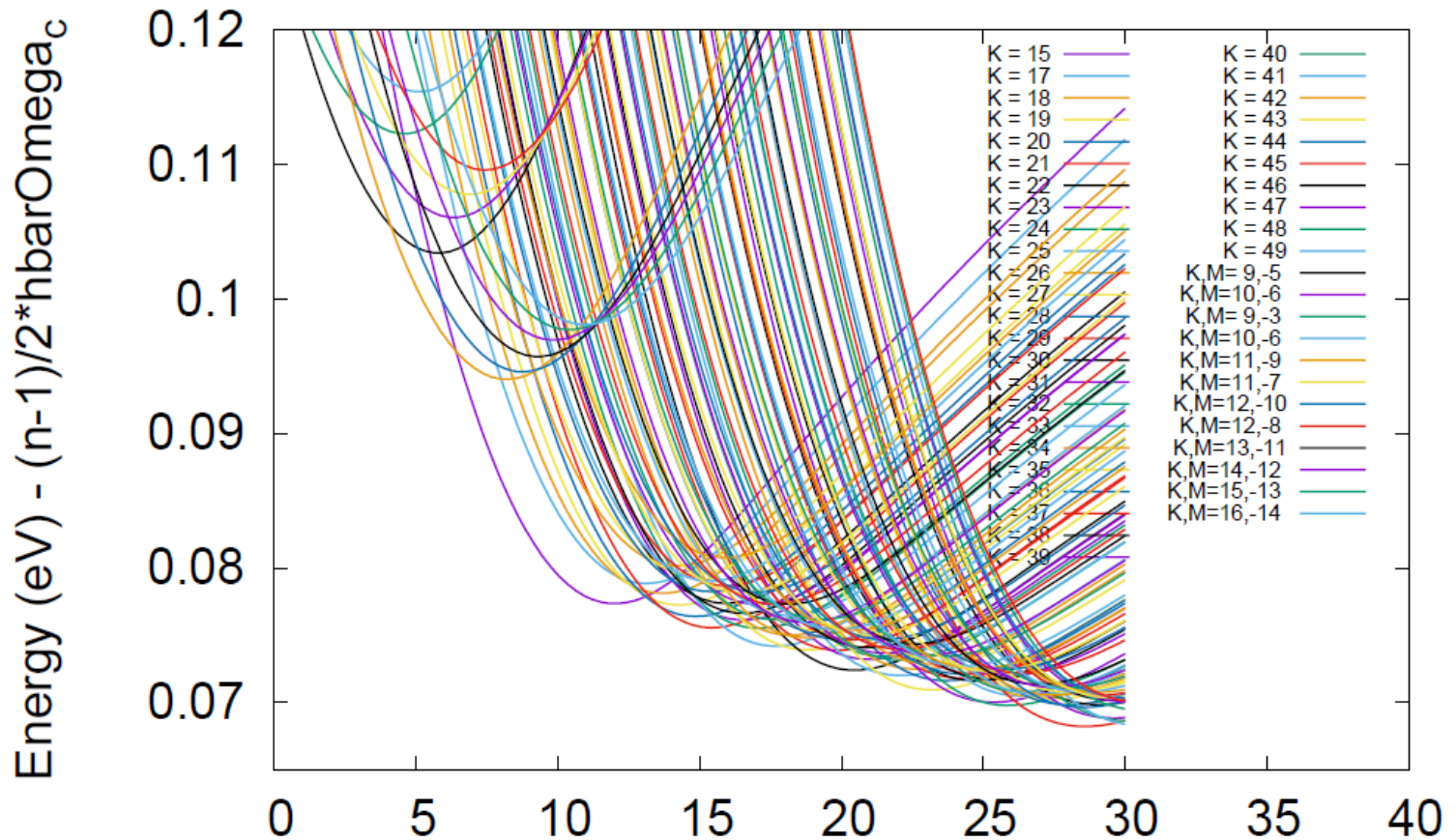
TABLE I. Sample list of identified N-body quantum Hall states in the lowest Landau level. M is the total relative azimuthal quantum number of Laughlin and Jain states identified by exact numerical diagonalization in a spherical geometry [6]. ν_{CF} gives the filling factor of identified QH states according to the Jain composite fermion picture, including a correction that accounts for the finite size shift associated with the spherical geometry. ν_{HS} is the calculated hyperspherical filling factor, given by Eq.(34). The final column gives a finite size correction to the hyperspherical filling factor.

Energy vs. Magnetic field



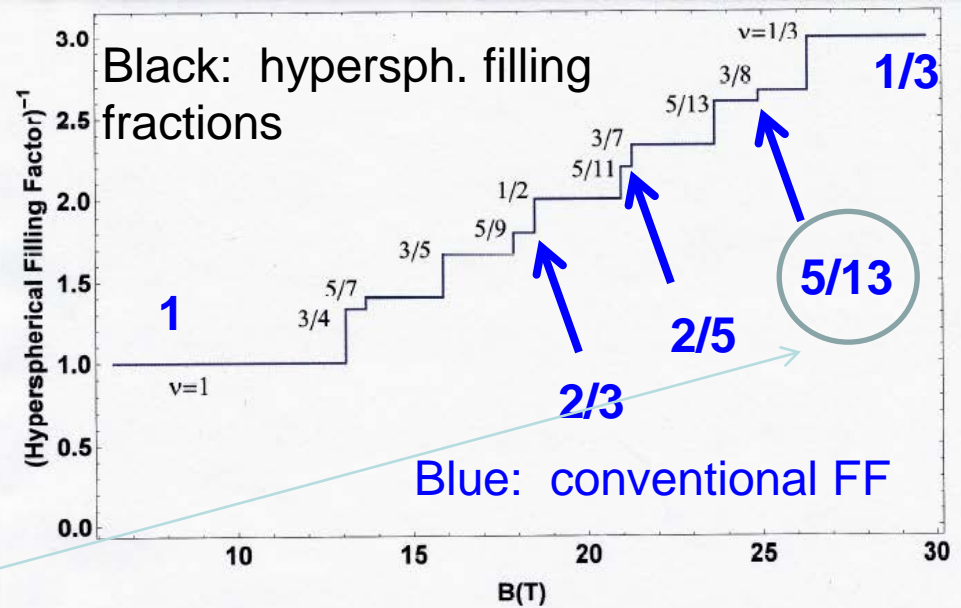
Energy spectrum after solving for the hyperradial vibrational degree of freedom, as a function of magnetic field. The B-field magnitude correlates with the maximum hyperradius used in the radial calculation according to the formula

Energy vs. Magnetic field

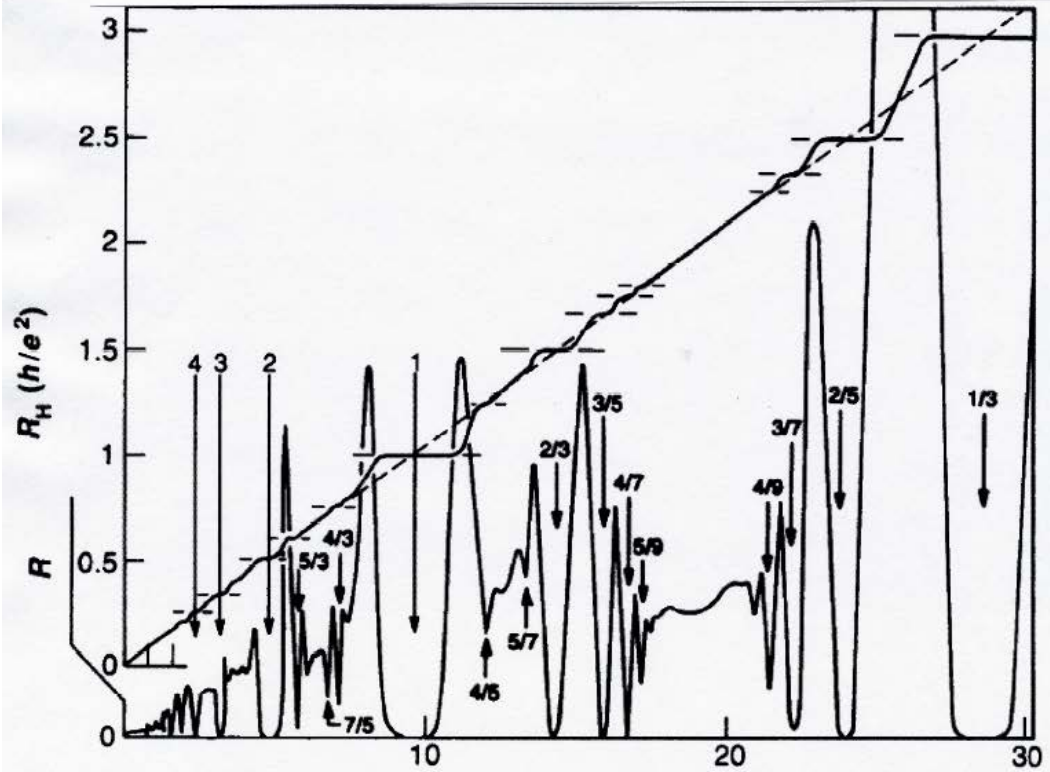


$R_{\max} = 2.65 \cdot \sqrt{B_{\text{field}}}$

“Devil’s Staircase” showing lowest energy state for 6 electrons with density, effective mass, and dielectric constant parameters appropriate for a typical GaAs experiment in the fractional quantum Hall effect.



Interestingly, the $5/13$ state that emerges from the 6 electron calculation ($M=-39$) is one state in particular that does not emerge naturally in the Jain composite fermion picture. On the Haldane sphere (for experts) it corresponds to $2Q=13$, with 1 completely filled composite fermion Landau level 0 + a partially filled Landau level 1 that holds the extra quasi electrons, which interact to form pairs. See Quinn&Quinn, SSSComm 2006



Fractional Quantum Hall Effect of Composite Fermions

W. Pan^{1,2}, H.L. Stormer^{3,4}, D.C. Tsui¹, L.N. Pfeiffer⁴, K.W. Baldwin⁴, and K.W. West⁴

¹*Department of Electrical Engineering, Princeton University, Princeton, New Jersey 08544*

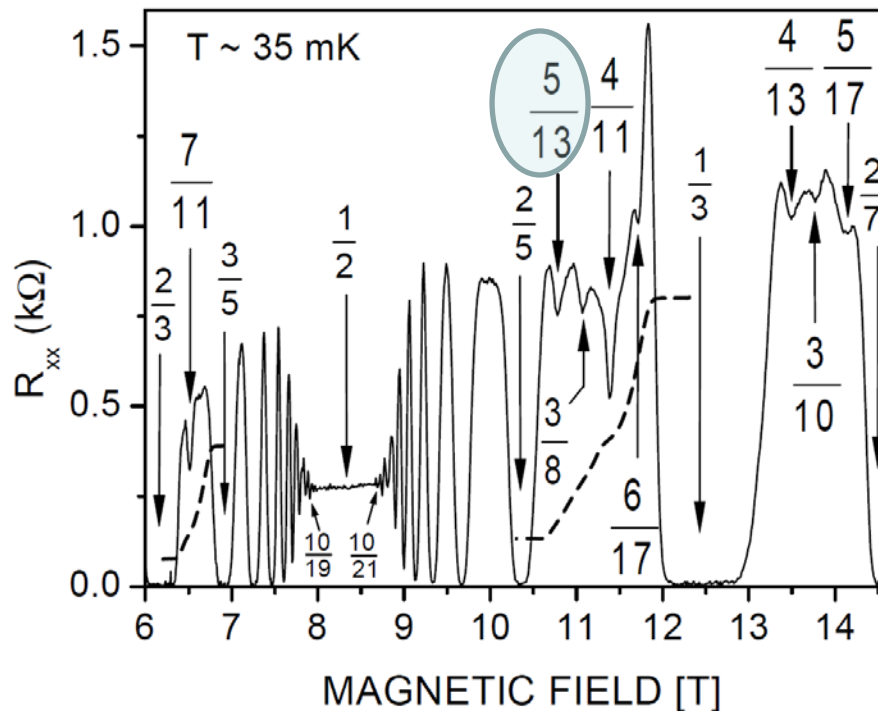
²*National High Magnetic Field Laboratory, Tallahassee, Florida 32310*

³*Department of Physics and Department of Applied Physics, Columbia University, New York, New York 10027*

⁴*Bell Labs, Lucent Technologies, Murray Hill, New Jersey 07974*

(January 13, 2014)

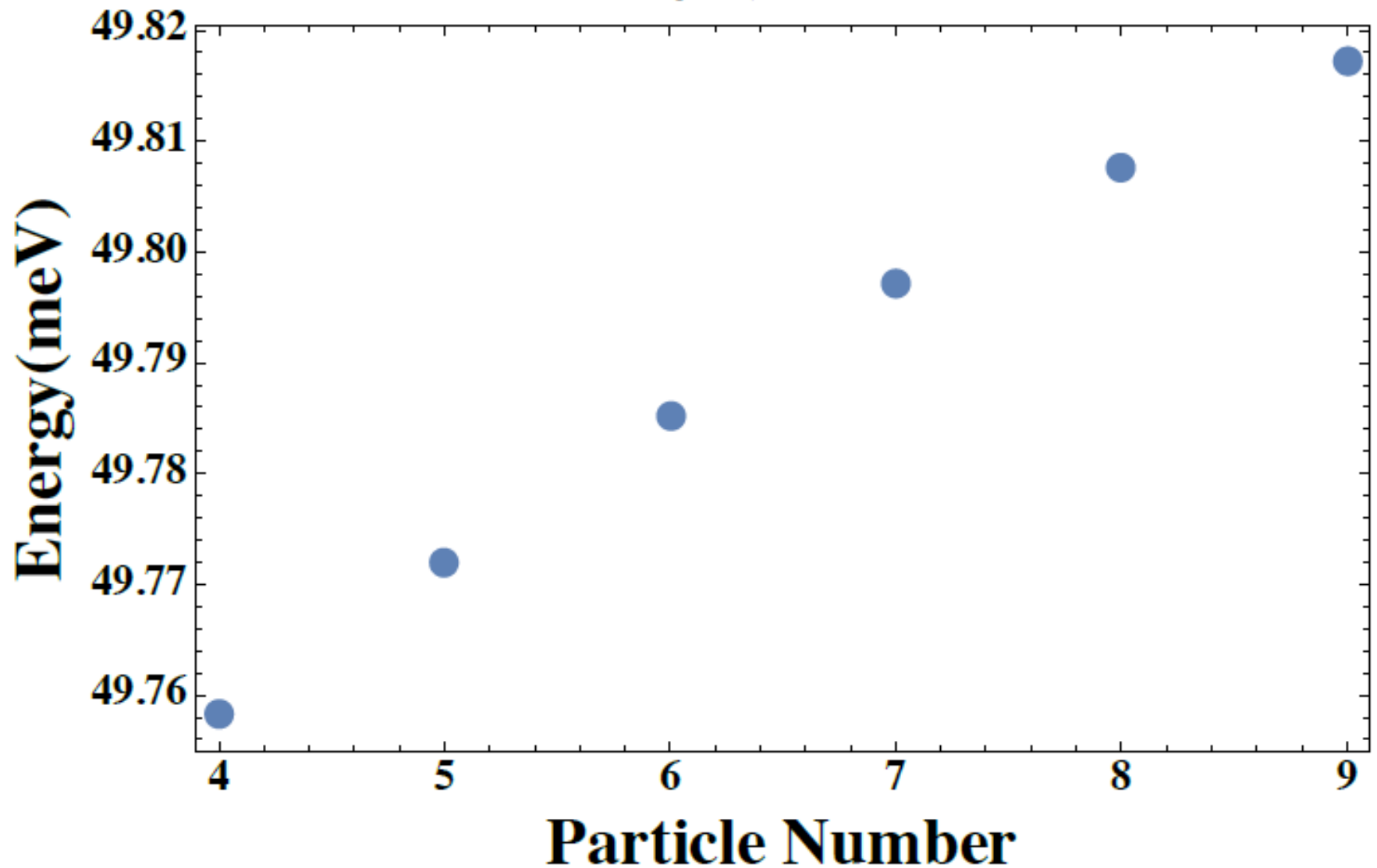
In a GaAs/AlGaAs quantum well of density $1 \times 10^{11} \text{ cm}^{-2}$ we observed a fractional quantum Hall effect at $\nu = 4/11$ and $5/13$, and weaker states at $\nu = 6/17, 4/13, 5/17$, and $7/11$. These sequences of fractions do not fit into the standard series of integral quantum Hall effects (IQHE) of composite fermions (CF) at $\nu = p/(2mp \pm 1)$. They rather can be regarded as the FQHE of CF's attesting to residual interactions between these composite particles. In tilted magnetic fields the $\nu = 4/11$ state



Experimental observation of some states that challenge the first-order composite fermion theory, in which the CF's are noninteracting;
condmat/0303429

Breathing mode signatures of the Laughlin 1/3 state, a prediction (preliminary):

$$\nu = 1/3, B = 29T$$



What have we learned, what can we conjecture, where are we going from here?

1. The adiabatic hyperspherical approximation is more accurate for the quantum Hall problem than for any other nonperturbative problem we have encountered to date. **In other words the hyperradius R is almost exactly separable from the other coordinates in this problem**
2. There appears to be a very strong correlation between the $\{K, M\}$ -manifolds representing observable fractional filling factors and the “**Exceptional Degeneracy**” of those manifolds. This suggests that it may be primarily a property of the **NONINTERACTING** electron gas that controls whether a given filling factor ν will give a FQHE resistivity plateau
3. As one looks at degeneracy patterns for more and more electrons, the degeneracy of angular momentum M is not so different from $M+2$ and $M-2$, etc. This suggests that possibly it could be relatively small numbers of electron droplets that are responsible for states that stand out so noticeably in the observed FQHE states
4. Note that one outcome is that for each M , viewed as a Hilbert subspace by itself, the eigenstates would be **EXACTLY THE SAME** even if there were no magnetic field present. This means that the same states (e.g. Laughlin $1/3$) can be formed even at $B=0$ with charged particles in a micro-trap.

Other directions to understand:

-- origin of fractional charge carriers, anyonic statistics, the $5/2$ state, etc.

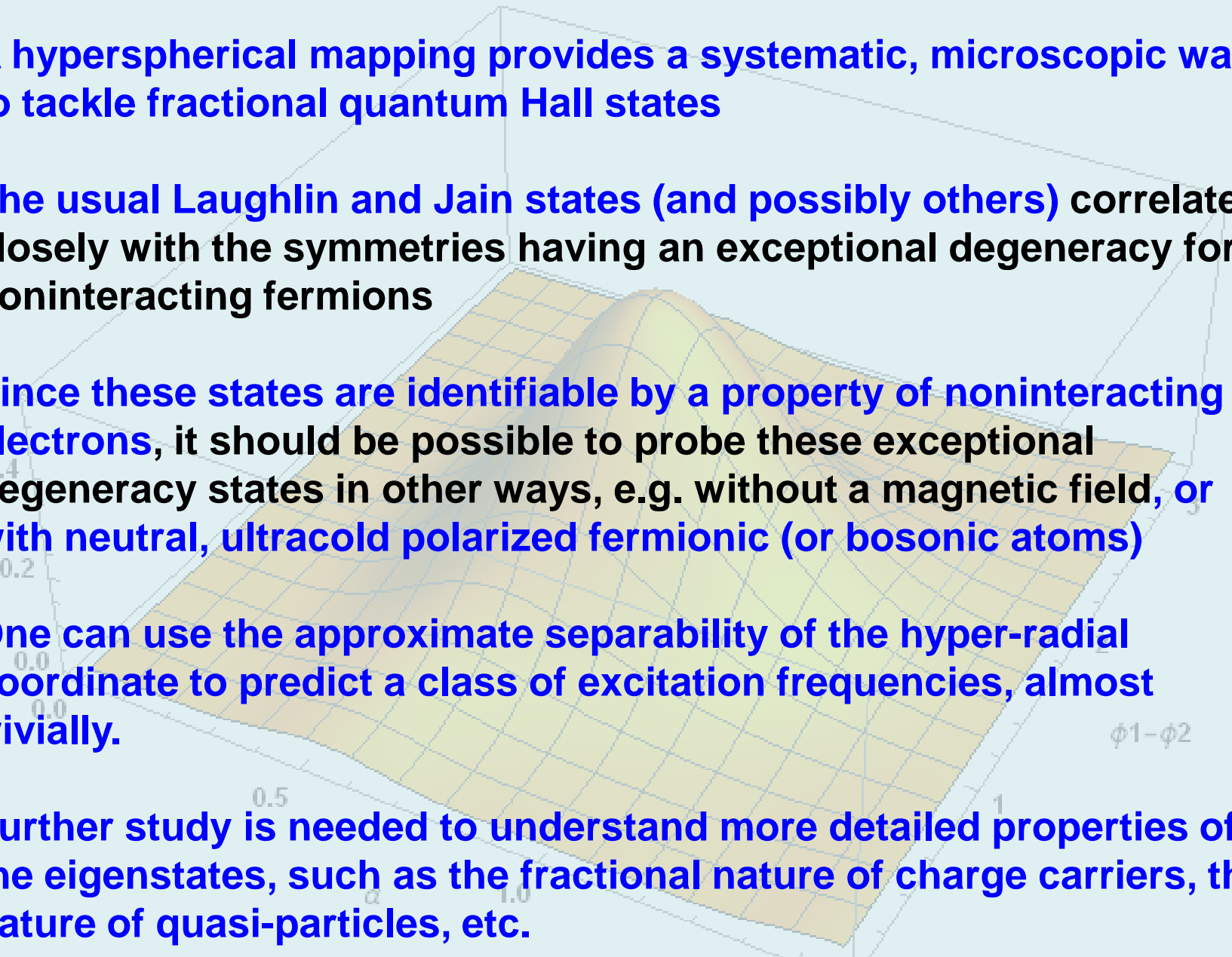
-- role and implications of entanglement and correlations

--connection with chaos (random matrix theory, semiclassical closed-orbit theory a la Gutzwiller, etc.)

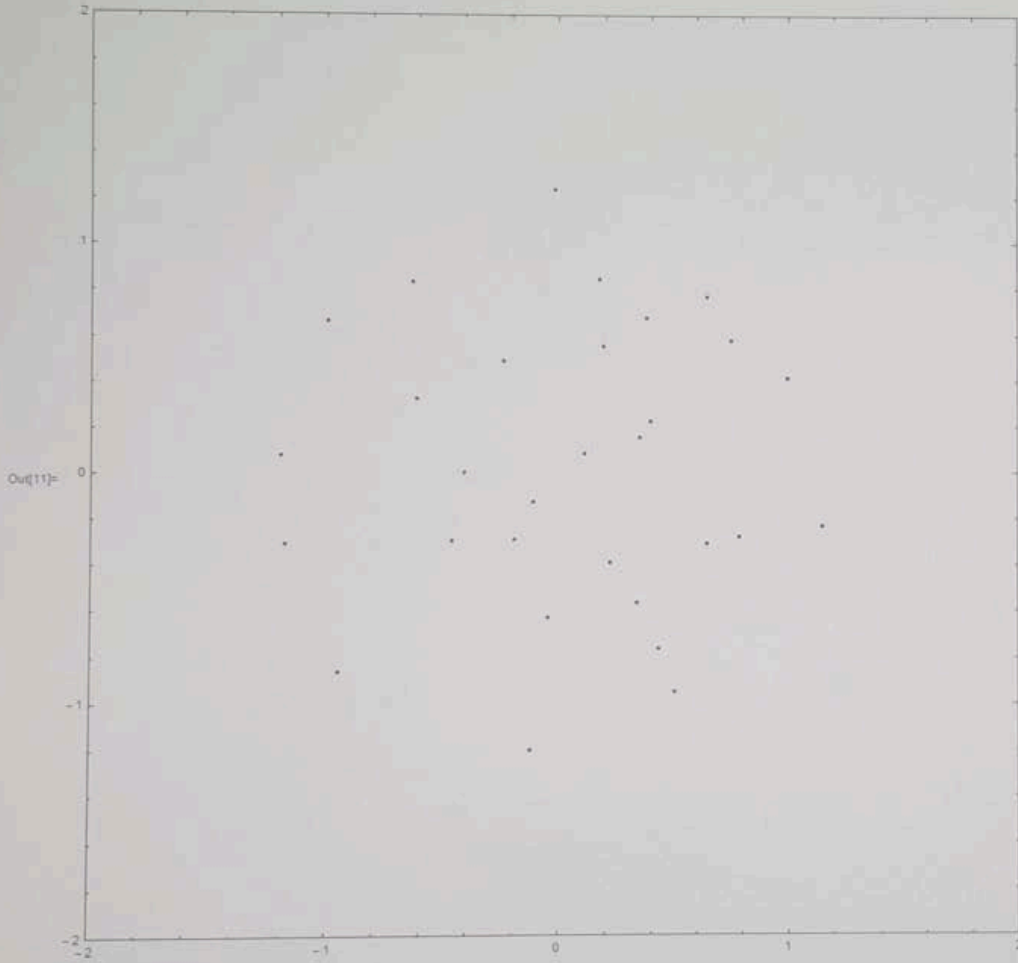
--conductance fluctuations in the Corbino geometry

-- predictions of novel spectroscopic signatures?

Conclusions

1. A hyperspherical mapping provides a systematic, microscopic way to tackle fractional quantum Hall states
 2. The usual Laughlin and Jain states (and possibly others) correlate closely with the symmetries having an exceptional degeneracy for noninteracting fermions
 3. Since these states are identifiable by a property of noninteracting electrons, it should be possible to probe these exceptional degeneracy states in other ways, e.g. without a magnetic field, or with neutral, ultracold polarized fermionic (or bosonic atoms)
 4. One can use the approximate separability of the hyper-radial coordinate to predict a class of excitation frequencies, almost trivially.
 5. Further study is needed to understand more detailed properties of the eigenstates, such as the fractional nature of charge carriers, the nature of quasi-particles, etc.
- 

```
amid = pos +  $\frac{vel \cdot h}{2}$ ;  
(*tab=Table[{xmid[[i]], ymid[[i]], {i, Length@pos}}];*)  
Do[amid[[i]] = force3[i], {i, Length@pos}];  
pos = pos + vmid h;  
vel = vel + amid h;},  
Frame -> True,  
PlotRange -> {{-size, size}, {-size, size}}
```



To change κ , B field, viewing range: change the following and the upper figure will dynamically change

In[12] = $\kappa = 0.5$;
B = 10;